Edible nano-encapsulated cinnamon essential oil hybrid wax coatings for enhancing apple safety against food borne pathogens

Yashwanth Arcot [a], Minchen Mu [a], Yu-Ting Lin [a], William DeFlorio [a], Haris Jebrini [b],
Angela Parry-Hanson Kunadu [c], Yagmur Yegin [d], Younjin Min [e], Alejandro Castillo [b],
Luis Cisneros-Zevallos [f], Thomas M. Taylor [g], Mustafa E.S. Akbulut [a,h,*]

[a] *Artie McFerrin Department of Engineering, Texas A&M University, College Station, TX 77843, USA*
[b] *Department of Food Science and Technology, Texas A&M University, College Station, TX 77843, USA*
[c] *Texas A&M Institute for Advancing Health Through Agriculture, College Station, TX, 77843, USA*
[d] *Massachusetts Institute of Technology, Civil and Environmental Engineering, Cambridge, MA 02139, USA*
[e] *Depart of Chemical and Environmental Engineering, University of California, Riverside, CA, USA, 92521*
[f] *Department of Horticultural Sciences, Texas A&M University, College Station, TX, 77843, USA*
[g] *Department of Animal Science, Texas A&M University, College Station, TX, 77843, USA*
[h] *Department of Materials Science and Engineering, Texas A&M University, College Station, TX 77843, USA*

ARTICLE INFO

ABSTRACT

Post-harvest losses of fruits due to decay and concerns regarding microbial food safety are significant within the produce processing industry. Additionally, maintaining the quality of exported commodities to distant countries continues to pose a challenge. To address these issues, the application of bioactive compounds, such as essential oils, has gained recognition as a means to extend shelf life by acting as antimicrobials. Herein, we have undertaken an innovative approach by nano-encapsulating cinnamon-bark essential oil using whey protein concentrate and imbibing nano-encapsulates into food-grade wax commonly applied on produce surfaces. We have comprehensively examined the physical, chemical, and antimicrobial properties of this hybrid wax to evaluate its efficacy in combatting the various foodborne pathogens that frequently trouble producers and handlers in the post-harvest processing industry. The coatings as applied demonstrated a static contact angle of $85 \pm 1.6°$, and advancing and receding contact angles of $90 \pm 1.1°$ and $53.0 \pm 1.6°$, respectively, resembling the wetting properties of natural waxes on apples. Nanoencapsulation significantly delayed the release of essential oil, increasing the half-life by 61 h compared to its unencapsulated counterparts. This delay correlated with statistically significant reductions ($p = 0.05$) in bacterial populations providing both immediate and delayed (up to 72 h) antibacterial effects as well as expanded fungal growth inhibition zones compared to existing wax technologies, demonstrating promising applicability for high-quality fruit storage and export. The utilization of this advanced produce wax coating technology offers considerable potential for bolstering food safety and providing enhanced protection against bacteria and fungi for produce commodities.

1. Introduction

In 2022, the global fruit and vegetable market, valued at $144 billion and growing annually at 5%, stands as a significant and robust industry with substantial economic impact worldwide (*Global Fresh Fruits and Vegetables Market Segmented,* 2023). Over 50% of agricultural fruit production is lost during various stages of produce handling and post-harvest treatments (Carmona-Hernandez et al., 2019). In addition to the reduced shelf life of these raw agricultural commodities, there exists a potential risk of foodborne illnesses. This risk stems from fruits and vegetables that are primarily consumed raw or only minimally processed, serving as vehicles for human microbial pathogens following pre-and/or post-harvest contamination (Bhardwaj et al., 2023; Mostafidi et al., 2020; National Food and Agriculture Incident Annex to the Response and Recovery Federal Interagency Operations Plans, 2019).

Many innovative treatment and storage techniques have been employed in recent years to extend the shelf life of fruits and vegetables (Adainoo et al., 2023; Banu A et al., 2020; S. Yang et al., 2012). To

---

counter the short lifespan of fruits and vegetables, one approach during post-harvest processing is the application of artificial wax coatings. This approach aims to decrease water loss through their skin, enhance protection against water and air-borne pathogens, and improve their external texture and appearance, making the fruits and vegetables glossy and more appealing to consumers (Fernández-Muñoz et al., 2022; Md Nor and Ding, 2020; Pashova, 2023). The use of paraffin wax to enhance the epicuticular surface waxes on fruits with smooth topography such as apples, cucumber, and pear has several advantages (Maringgal et al., 2020). With the Generally Recognized as Safe (GRAS) status provided to paraffin waxes by the U.S. Food and Drug Administration (FDA), safety is ensured, and confidence is imparted to consumers and industry professionals regarding its use in fruit coatings and other food-allied applications (Food and Drug Administration, CFR - Code of Federal Regulations Title 21, Section-175.250, 2023). Additionally, paraffin waxes are inexpensive and have relatively low melting points (typically ranging between 48 and 66 °C), facilitating its application to fruits, ensuring a uniform coating without damaging the fruits (Joshi et al., 2021). The use of hot-melt paraffin waxes to dip coat apples and pears is a straightforward industrial practice to provide a protective barrier around the fruits and aid in improving their shelf life and preventing water loss (Muthuselvi et al., 2020).

Despite the presence of protective wax coverings, fruits and vegetables remain susceptible to pathogenic microbes throughout different post-processing stages before they reach consumers. Most of the artificial epicuticular wax coatings achieved by dip-coating lack roughness at the micrometer/nanometer scale, promoting a Wenzel state of wetting (Aguilar-Morales et al., 2019; Gennes et al., 2004). In addition, these wax coatings exhibit water contact angles typically ranging between 90° and 100° (Bohinc et al., 2022; Hall, 1966; Oliveira Filho et al., 2022). This property invites a higher concentration of bacterial attachment and biofilm formation, attributable to hydrophobic-hydrophobic interactions between the bacterial cell wall and the substrate, along with physiochemical adsorption facilitated by the elimination of the interfacial water layer (Cai et al., 2019; Fernandes et al., 2014; Oh et al., 2018; Rosenberg and Kjelleberg, 1986; Sheng and Zhu, 2021; Yuan et al., 2017). Moreover, imperfections, injuries, and blemishes on the wax surface, which can occur during storage and transport, can serve as entry points for pathogens, thereby increasing fruit vulnerability to contamination.

To overcome these challenges, researchers have proposed the use of composite wax structures with chitosan derivatives (El-Sakhawy et al., 2023; Ruan et al., 2022; Tang et al., 2022), chemical fungicides (Fei et al., 2021; Palou and Pérez-Gago, 2021) and essential oils (Bashir et al., 2023; Yaashikaa et al., 2023). Essential oils with GRAS status are excellent ability to combat bacterial and fungal contaminants and/or infections (Reyes-Jurado et al., 2022; Rosol et al., 2023). With the presence of bioactive terpenes, alcohols, and aldehydes, essential oils contribute to enhancing cell wall permeability, inducing cell wall degradation, leading to the leakage of cellular components, and ultimately resulting in the mortality of pathogenic species (Chouhan et al., 2017; Ju et al., 2022). In recent years, numerous researchers have utilized essential oil-based food sanitization techniques to enhance shelf life and provide superior protection (Gao et al., 2024; Ju et al., 2023; B. Li et al., 2023).

Essential oils, with their inherent volatility and strong aroma, as well as the less stable nature of some phytochemicals, cannot be used directly on fruits by themselves (Phosanam et al., 2023). Hence, researchers have suggested the use of innovative techniques of harnessing them onto the fruits. Recently, many researchers have explored the integration of essential oil-based nanotechnology into wax coatings on fruits (Chi et al., 2019; Miranda et al., 2022; Oliveira Filho et al., 2022; Rux et al., 2023). This innovative approach aims to enhance the shelf life of fruits, while also mitigating the risk of cross-contamination throughout the various stages of production and processing, ensuring optimal fruit quality for the end consumer.

Despite the effectiveness of these novel composites, no previous studies have focused on the nanoencapsulation of essential oils to achieve delayed release, decreasing aroma intensity and mitigating microbial cross-contamination during industry-typical conditions of post-harvest processing and storage. Additionally, the exploration of novel strategies, such as incorporating encapsulated essential oils into commercial waxes, to effectively control the proliferation and cross-contamination of these foodborne pathogens, which can be transmitted through air and water during post-harvest and storage processes, remains largely unexplored.

In present research, we propose a novel, facile and industrially scalable paraffin wax-based dip coating technique to decrease bacterial foodborne pathogen proliferation on produce surfaces by extended release of antimicrobial agents on red apples. For bench scale coating and characterization convenience, we used a filter paper, quantitative grade as a proxy surface to the fruit's skin to estimate the physical characteristics and efficacy of the hybrid coating formulations. To confer antimicrobial characteristics to the wax coatings, we utilized cinnamon bark essential oil (CEO; purchased from Viva Doria, Monroe, Washington, USA), known for its antibacterial and antifungal properties (X. Chen et al., 2021; Lucas-González et al., 2023; Purkait et al., 2020). In our research whey protein concentrate was used as nanocarrier for CEO. Whey protein is known to offer higher colloidal and chemical protection to the encapsulated active ingredients and excellent barrier characteristics for the aroma of CEO (H. Chen et al., 2019; Livney, 2010). The effectiveness of these hybrid coating technologies was studied through various physical and chemical surface characterization methods, release profile analysis in aqueous medium, and several microbiological assays.

2. Materials and methods

2.1. Cinnamon essential oil characterization

To obtain a comprehensive understanding of the chemical composition within the commercially procured CEO, Gas Chromatography-Mass Spectroscopy (GC-MS) was employed. This analysis involved the utilization of a Trace GC Ultra (Thermo Scientific, Waltham, MA, USA) integrated with an MS (DSQ II, Thermo Scientific, Waltham, MA, USA), employing a DB-5MS capillary column (30 m × 0.25 mm × 0.25 μm, containing the stationary phase). Helium gas functioned as the mobile phase, facilitating the transport of volatile constituents. The initial column temperature was set at 50 °C (held constant for 2 min to eliminate the solvent), followed by a consistent increase at a rate of 6 °C/minute up to 250 °C.

2.2. Preparation of nano-encapsulated essential oils

We optimized the formulation by experimenting with various ratios of whey protein concentrate used for encapsulation and the bioactive CEO. Ultimately, we selected the formulation that resulted in the highest entrapped CEO yield at the conclusion of the freeze-drying process. The nanoparticle synthesis procedure involved the dissolution of 0.075 g whey protein concentrate (Natural Force, Jacksonville, FL, USA) into a glass vial containing 10 mL deionized (DI) water. To ensure the complete dissolution of the whey protein in deionized (DI) water, the mixture was agitated vigorously. Subsequently, 0.075 g of CEO was added dropwise to the protein solution under constant agitation. To homogenize the resulting mixture, probe sonication was employed at a frequency of 24.8 Hz and a power intensity of 40%, maintained for a duration of 2 min. Following this, the colloidal suspension was set aside to equilibrate to room temperature on the laboratory bench. Once cooled, the suspensions were transferred to 15 mL Falcon tubes and immediately subjected to lyophilization (freeze-drying) for 48 h using a Labconco 4.5 L freeze dryer (Labconco Corp., Kasnsas City, MO, USA). The prepared particles (EO-NE particles) were stored at 25 °C on a lab-bench.

2.3. Preparation of specimens used for coating procedure

All coating procedures were conducted using pristine filter papers (quantitative grade, Fp 494, Avantor, Radnor, PA, USA). For release kinetics studies, circular filter paper was cut into four parts, forming four quarter circles with a surface area measuring 5 cm^2. To evaluate bacterial growth kinetics in various media, the filter papers were cut into rectangular strips of 6 cm × 2 cm instead of quarter circles. These strips were then rolled, and the ends of the strips were securely fastened to form a hollow cylindrical structure. For performing the disc diffusion assay (Kirby-Bauer method), the filter papers were cut into 6 mm pellets using a punching machine. These pristine filter paper pieces were coated with different formulations and utilized in various assays as described below.

2.3.1. Wax coated samples

To prepare these coatings 40 g of paraffin wax (Sigma-Aldrich, Burlington, MA, USA) was taken in a 100 mL beaker and heated to 70 °C. Once the wax was completely melted, the filter paper piece was submerged into the melted wax and removed immediately. The wax-coated pieces (PW) were allowed to dry at room temperature.

2.3.2. Unencapsulated cinnamon-essential oil embedded wax coated samples

These samples were developed by melting 40 g wax (in 100 mL glass beaker) at 70 °C to which 0.2 g CEO (Naturevibe Botanicals, Rahway, NJ, USA) was added dropwise under continuous stirring using a glass rod. Pristine filter paper pieces were immersed into the unencapsulated CEO dispersed wax mixture, promptly removed, and subsequently air-dried at room temperature. These samples are identified as EO-PW substrates.

2.3.3. Encapsulated cinnamon-essential oil embedded wax coated samples

These samples involved CEO-encapsulated wax coatings (termed EO-NE-PW). Like the aforementioned procedure, 40 g of paraffin wax was heated to 70 °C to create a molten wax phase. Subsequently, 0.8 g of finely powder (by mechanically breaking the lumps using a spatula) EO-NE particles were gradually introduced to the wax melt with continuous stirring using a magnetic stirrer. The pristine filter paper pieces were dipped, immediately removed, and dried at 25 °C. Note that to prepare each batch of EO-NE-PW samples, fresh mixtures of EO-NE and paraffin wax were utilized, as the integrity of the nanoparticles was destroyed with time in wax melts.

2.4. Physical and chemical characterization of freeze-dried cinnamon essential oil embedded nanoparticles

2.4.1. Nanoparticles size and surface charge

To characterize the hydrodynamic diameters of nano-encapsulates as prepared and after freeze-drying followed by redispersing in DI water at same concentration levels, and to understand the stability of the colloidal suspension, ζ-potential and dynamic light scattering (DLS) was performed at 25 °C. The prepared samples were diluted 100 times using DI water before performing the DLS (using a Zetasizer ZS90 analyzer; Malvern Instruments, Ltd., Westborough, MA, USA) to ensure the passage of light through the sample and to avoid multiple light scattering.

2.4.2. Visual characterization of nanoparticles

High-resolution transmission electron microscopy (TEM) and scanning electron microscopy (SEM) images were acquired to ascertain the shape and dimensions of the nanoparticles in their solution state (before freeze-drying) and following the freeze-drying process. TEM images were captured using a FE-TEM (G2 F20 ST, FEI Tecnai, Hillsboro, OR, USA). Prior to TEM analysis, the nanoparticle solutions were appropriately diluted by a factor of ten using deionized (DI) water at ambient temperature. Subsequently, 5 μL of the suspension and a staining solution (1% uranyl acetate) were individually deposited onto a 300-mesh copper grid for a duration of 45 s each. Following this, the grid was allowed to air-dry at room temperature over the course of a night prior to conducting TEM observation (Lin et al., 2023; Mu et al., 2023). The freeze-dried nanoparticle powder was characterized using SEM (Tescan LYRA-3 Model GMH) under high-resolution mode at 93.3 k × . Prior to image characterization, the nanoparticle powders were coated with Pt/Pd (5 nm thickness) using a sputter coater (Cressington 208HR, Cressington Scientific Instruments, Watford, UK) to enhance the conductivity of the samples and reduce charging (Arcot et al., 2021; Liu et al., 2021).

2.4.3. Chemical characterization of nanoparticles

To validate the successful encapsulation of CEO within the whey protein matrix, Attenuated Total Reflectance Fourier Transform Infrared (ATR-FTIR) spectroscopy was conducted using an IRPrestige-21 instrument (Shimadzu Corp., Kyoto, Japan) within the wavenumber range of 400 cm^{-1} to 4000 cm^{-1}. Three distinct samples were analyzed: liquid essential oil, whey protein concentrate powder, and freeze-dried EO-NE powders. The collected spectral data were plotted using OriginPro 2021 software and functional group analysis was performed to elucidate the encapsulation process.

2.5. Physical characterization of the coated filter-paper samples

2.5.1. Wetting behavior and contact angle

To compare the wetting behaviors of PW, EO-PW and EO-NE-PW, static-contact angles (SCA) and dynamic contact angles: advancing and receding contact angles were characterized. The images were captured using an OCA11 goniometer/tensiometer (DataPhysics Instruments, Charlotte, NC, USA). SCA was measured utilizing the sessile drop technique employing 5 μL deionized (DI) water droplets. To facilitate real-time video recording of advancing and receding contact angles, 5 μL DI water pendant droplets were brought into firm contact with the surface of the substrate. An additional 15 μL was incrementally added to the droplet, ensuring continuous contact with the substrate at a controlled rate of 0.5 μL/s, followed by withdrawal at the same rate until the final droplet volume reached 5 μL. A lag time of 30 s was consistently maintained between the addition and withdrawal of the DI water. This systematic approach allows for precise determination of contact angles and facilitates the observation of dynamic wetting behaviors (DeFlorio et al., 2023). The measurement procedure was replicated at least six times before reporting the contact angle values.

2.5.2. Surface characterization

To comprehend the surface morphology and internal structure variations among wax coatings with distinct formulations, SEM was employed. The samples were subjected to sputter coating followed by image capture. To obtain cross-sectional insights into the wax coatings, the wax-coated filter papers (different formulations), were precisely sectioned into 1 mm wide strips. These strips were subjected to freeze-drying prior to sputter coating and both surface and cross-sectional imaging was conducted. Furthermore, for a comprehensive understanding of the elemental distribution across the surface of the wax coatings, Energy-dispersive X-ray spectroscopy (EDX) was employed using an Oxford instrument (NanoAnalysis, Concord, MA, USA). Following the capture of low-magnification SEM images, EDX elemental mapping was performed at an accelerating voltage of 10 kV. This technique enabled a detailed analysis of the elemental composition within the regions of interest. The data were reported after replicating the respective characterizations three times.

2.6. Quantitative analysis of cinnamon essential oil

2.6.1. Calibrating cinnamon essential oil via UV–visible absorbance

To comprehend the relationship between concentration and

absorbance values, CEO was dispersed in 10% ethanol solutions across varying concentrations. Following this, the solutions were subjected to UV–visible spectroscopic analysis employing a UV–Vis spectrophotometer (UV-1800, Shimadzu Corp., Columbia, MD, USA). A quantity of 3 mL of each solution was placed within a quartz cuvette for the analysis. The UV–Vis instrument facilitated scanning within the wavelength range of 800 to 200 nm (before this step, a background scan was conducted using a pristine 10% ethanol solution without any essential oil). The peak intensity at 294 nm, predominantly occurring due to π to π* transitions in of cinnamaldehyde was recorded for analysis (Cox et al., 2021). This procedure was replicated three times at each concentration level. Using the collected data, a calibration scatter plot was constructed, correlating the concentration of CEO against the respective absorbance values.

2.6.2. Calculating the encapsulation efficiency and percent recovery after freeze-drying

10 mL of the prepared nanoparticle suspension underwent vigorous centrifugation using the AccuSpin 400 Benchtop Centrifuge (Fisher Scientific, Waltham, MA, USA) at $15\,000 \times g$ for 45 min. This ensured the settling of all essential oil encapsulated by whey protein, resembling a distinct pellet at the bottom of the centrifuge tube. 1 mL of supernatant liquid was obtained, and subsequently diluted by a factor of 100. The absorbance was measured using the UV–Visible spectrophotometer, allowing the calculation of the concentration of unencapsulated CEO after adjusting for proper decimal placement. The encapsulation efficiency was determined using the provided formula (1a).

Encapsulation efficiency (EE)%= (1-(CEO in supernatant /Initial CEO used for EO-NE preparation)) × 100 (1a)

In addition, the EO-NE-PW particles were dispersed in deionized (DI) water and diluted by a factor of 1000. Subsequent absorbance measurements were obtained using the UV–Visible spectrophotometer. Calculations of CEO concentration encapsulated post freeze-drying were then obtained; percentage recovery of CEO following freeze-drying was calculated using the given formula (1b).

Percentage recovery %= (CEO in EO-NE-PW/ Initial CEO used for nanoparticle preparation) × 100 (1b)

2.6.3. Studying the release kinetics of cinnamon essential oils

Two filter papers with a surface area of 5 cm^2, were coated with wax-dispersed cinnamon essential oils (EO-PW) and EO-NE nanoparticles-dispersed wax (EO-NE-PW), respectively. These coated filter papers were then carefully enclosed within dialysis bags (pore size of 12–14 kD; Spectrum, Spectra/Por, St. Louis, MO, USA) and supplemented with 10 mL of deionized (DI) water. The dialysis pouches were sealed using sealer clips on both ends. 990 mL of DI water was introduced into a glass beaker, serving as the immersion medium for the dialysis pouches. The pouches were submersed in each beaker containing the DI water. To prevent evaporation of DI water and dissolved essential oil, the beaker was covered with aluminum foil.

To facilitate a quantitative comparison, a control experiment aimed at demonstrating release kinetics of CEO from EO-NE via the dialysis pouch (12–14 kD), a separate experiment was conducted. 0.16 g of EO-NE particles were dispersed in 10 mL deionized (DI) water and introduced into a dialysis pouch. Both the ends of the pouch were securely sealed using bag sealer clips. The dialysis bag was then carefully immersed into a beaker containing 990 mL DI water.

UV–visible absorption spectrograms were recorded by introducing 3 mL of liquid from the quartz cuvette. The cuvette contents were then returned to their original state after the measurement was completed. The readings were systematically captured at predetermined time intervals of 1, 2, 8, 16, 24, 48, 96, 168, 216, and 336 h. This experimental protocol was repeated three times before reporting.

2.7. Microbial assessment of essential oil-based nanoparticle embedded wax coatings

2.7.1. Preparation of bacterial cultures: inoculation procedures

All abiotic reagents employed for bacterial culturing, inoculation, and experimentation underwent autoclaving at 121 °C for 45 min to ensure complete sterility and eliminate any potential bacterial contamination. The study focused on two bacterial foodborne pathogens: the gram-negative facultatively anaerobic regularly shaped rod *Escherichia* coli O157:H7 (American Type Culture Collection [ATCC] 700 728, Manassas, VA, USA) and the gram-positive facultative anaerobic coccoid *Staphylococcus* aureus (ATCC 13565).

Bacterial colonies were extracted from the prepared trypticase soy agar (TSA) slants using method outlined previously (DeFlorio et al., 2023). These colonies were then suspended in 9 mL of sterile trypticase soy broth (TSB) and incubated at 37 °C with the cap of the Falcon tube (15 mL) slightly loosened to allow for proper air exchange. After 24 h of incubation, a loop (10 μL) of these cultures were transferred into a fresh TSB solution. After a further 24 h of incubation, cultures were subjected to centrifugation (for 15 min at $15\,000 \times g$). The resulting supernatant was carefully removed, and fresh TSB was introduced. This process was repeated thrice to facilitate the removal of cellular waste, enzymes, and debris from the bacterial suspensions. These washed bacterial pellets were subsequently referred to as second transfer bacterial pellets in subsequent discussions. The second transfer bacterial pellets were dispersed in ultra-pure grade phosphate-buffered saline (PBS) with a concentration of 10 mM and a pH of 7.4. Subsequently, they underwent decimal dilution, followed by plating on tryptic soy agar (TSA; Becton, Dickinson and Company (Franklin Lakes, NJ, USA)-loaded Petri dishes. Upon plating, the bacterial populations were quantified after a 24-h incubation at 37 °C, revealing counts of 9.0 ± 0.04 log$_{10}$ CFU/mL and 9.0 ± 0.03 log$_{10}$ CFU/mL for *E. coli* and *S. aureus*, respectively.

2.7.2. Effectiveness and endurance of encapsulated cinnamon-essential oil embedded wax coatings

All the substrates utilized were in the form of hollow cylindrical strips with identical dimensions. Two distinct protocols were implemented in this study. Initially, to assess the anti-bacterial efficacy of hybrid coatings when exposed to bacterial suspensions, we conducted a comparison of the growth kinetics between EO-NE-PW substrates and pristine PW substrates. Subsequently, to evaluate the endurance of the coatings over extended periods, we compared EO-NE-PW with EO-PW coatings. Hence, two individual control benchmarks were utilized namely PW and EO-PW coatings in comprehending the effectiveness of EO-NE-PW coatings.

When evaluating the endurance of the EO-NE-PW coatings, the two substrates, namely EO-PW and EO-NE-PW, were immersed in sterile DI water solutions for 72 h. Subsequently, they were removed and gently washed to eliminate any loosely attached essential oils to the outer layers of the wax substrates before monitoring the growth kinetics.

2.7.3. Bacterial growth monitoring

The growth kinetics of the bacterial cultures were monitored by assessing the optical density (OD) at 600 nm using a BioTek Cytation 5 (BioTek Instruments, Inc., VT, USA). All measurements were conducted within 12-well plates (ThermoFisher Scientific). Hourly readings were taken after subjecting the well plate to a 15 s of orbital shaking.

The second transfer suspensions of both *E. coli* and *S. aureus* underwent 1000-fold dilution and subsequently dispersed in both sterile TSB and PBS and subjected to OD measurements to obtain control growth curves.

The assessment of growth kinetics in the presence of various coatings involved positioning three replicates of hollow cylindrical filter paper strips coated with these materials into separate well columns. These

hollow cylindrical strips were positioned within the wells longitudinally and unobstructed light passage was ensured. Subsequently, 3 mL of these diluted suspensions (in TSB and PBS) were introduced into the wells that contained the aforementioned paper strips. This approach aimed to facilitate maximum interaction between the bacterial suspension and the coatings, thereby enabling a comprehensive investigation into the influence of the released EO on bacterial growth dynamics. After the subtraction of the corresponding background values, the OD measurements were documented, and the growth kinetics were comprehensively studied.

To precisely quantify bacterial populations within the well plates both before and after conducting OD measurements, a decimal dilution technique followed by plating on Petri-films (3 M, St. Paul, MN, USA) was executed. The plating procedure was carried out for several distinct bacterial suspension samples including, the initial concentration at t = 0 h (prior to commencing the OD experiment), the concentration at the 24 h time point following bacterial inoculation in PBS and TSB, as well as the bacterial inoculums in PBS and TSB with the presence of various coating substrates, all aliquoted from the 12-well plate. The bacterial quantifications were repeated three times before reporting.

2.7.4. Quantification of bacterial attachment through shaker plate assay

The second transfer bacterial pellets were resuspended in 10 mL of PBS. These suspensions were subsequently subjected to a 10-fold dilution process. To prepare the experimental samples, 30 mL of these diluted suspensions were transferred into 50 mL Falcon tubes. In one set of Falcon tubes, PW was introduced, while in another set EO-NE-PW (of the same size) was used. The Falcon tubes containing the suspensions and filter papers underwent agitation on a shaker plate operating at 1000 rpm for a duration of 1 h. Following agitation, the samples were carefully retrieved, gradually immersed in sterilized DI water multiple times to eliminate any bacteria that were loosely bound or unbound. Subsequently, these samples were immersed in 10 mL PBS solution and subjected to vigorous agitation for a period of 5 min, ensuring complete removal of all bound bacteria. The bacterial suspensions, now containing the detached bacteria, underwent a series of dilutions. These diluted suspensions were then plated on TSA for the purpose of quantifying the bacterial populations. This comprehensive procedure was consistently replicated three times for both *S. aureus* and *E. coli* isolates.

2.7.5. Disc diffusion assay for monitoring fungal proliferation

To record the zone of inhibitions imparted by hybrid wax coatings, an assay like the Kirby-Bauer disk diffusion assay was used (Gautam et al., 2013; Tao et al., 2020; Uğur Tutar, 2020). Fungal mycelia were collected from refrigerated agar stocks of *Aspergillus flavus* (*A. flavus*) and dispersed in malt extract broth (MEB, 15 g/L), which was sterilized by autoclaving. After 4 h of incubation at 37 °C, mycelia-laden cotton swabs were gently applied to the solid surface of malt extract agar (MEA) with the depth of the agar being maintained at 4 mm. Filter paper substrates, namely PW and EO-NE-PW, were sectioned into 6 mm discs and positioned on separate halves of the MEA plates, ensuring optimal contact with the agar surface. Plates were then incubated for 10 days at 37 °C, and images were captured using a Panasonic H-HAS12035 digital camera on days 2, 3, 4, 6, 7, 8, and 10.

2.8. Observation of visual appearance of hybrid wax coatings on produce

To perform a comprehensive visual analysis of PW, EO-PW, and EO-NE-PW coatings, red apples were selected as the substrate of interest. The concentrations of CEO within the wax coatings were maintained consistent with the fabrication technique outlined above. Prior to application of these coatings, the apples (purchased from the local grocery store, Bryan, TX) were washed with chloroform to remove the pre-existing wax on the fruits. The paraffin wax formulations (both pristine paraffin wax and paraffin wax dispersed with CEO), were heated to 70 °C. Apples, stripped of their natural waxes, were dipped into the formulations and promptly removed. EO-NE particles were dispersed in paraffin wax formulations by vigorous agitation using magnetic stirring. The red apples were subsequently dipped and immediately removed. Additionally, precautions were taken to prevent any dripping of molten wax droplets by thoroughly shaking the apples after the coating application. The coatings were subsequently subjected to visual assessment using a Panasonic H-HAS12035 digital camera.

2.9. Statistical analysis

Statistical analysis was employed to assess the significance of the developed technology in each assay and characterization within the study versus an appropriate control. When both static and dynamic water contact angles were quantified for each substrate, an analytical framework encompassing One-way Analysis of Variance (ANOVA) was implemented. Tukey's post-hoc test was carried out, with the independent variable in these analyses being the substrate type. For the calibration of the concentration of CEO against absorbance, linear fitting was performed using the Origin 2021 software. The resulting linear fitting parameters were then compared to Beer's Lambert law to derive the relevant constants (Bouaziz et al., 2021).

The assessment of release kinetics was completed by adopting the mathematical equations employed by Bae et al., and the resultant fitting parameters were obtained (Bae et al., 2022). To assess bacterial growth kinetic parameters, a 3-parameter sigmoidal fitting model, utilizing re-parametrized Gompertz equation was executed (Science, 1990; Tjørve and Tjørve, 2017). The fitting process was carried out by defining the fitting model and executing the fitting using the software tool Origin 2021. For the statistical quantification of the bacteria in the media, one-way ANOVA was employed with the contact substrate being the quantity of interest in the Tukey's post-hoc test.

In addition, while conducting the shaker plate assay, a comprehensive analytical approach was embraced. Through the application of two-way ANOVA, the interaction of factors was systematically analyzed. Tukey's post-hoc test was carried out with the independent variables defined as the substrate type used and the genus of the bacterium.

Finally, statistical significance of the zones of inhibition measurements was calculated when PW and EO-NE-PW were in contact with agar petri plates laden with *A. flavus*. This assessment was conducted using a one-way ANOVA, with the zone of inhibition as the independent variable in the Tukey's post-hoc test.

3. Results and discussion

3.1. Chemical constitution of cinnamon essential oils

Several volatile bioactive constituents found in cinnamon essential oils, such as cinnamaldehyde and eugenol, contribute significantly to their antibacterial and antifungal properties (Ali et al., 2005; S. S. Cheng et al., 2008). Therefore, characterizing the composition of CEO is crucial to determine the presence and concentration of these phenolic compounds. Analysis revealed that the commercially purchased cinnamon essential oil contained 67.18% *trans*-cinnamaldehyde and 3.22% eugenol. Supplementary Material Table S1 provides details of other constituents along with their percent relative abundance and retention time. This data aligns consistently with previously reported literature on the constituents of cinnamon essential oil (Alizadeh Behbahani et al., 2020).

3.2. Characterization of structural and interfacial properties of nano-encapsulated essential oils

Studying the morphology, size, and size distribution of nano-encapsulated essential oils is crucial in formulation development as these characteristics significantly influence the release behavior, stability, and bioavailability of the encapsulated oils (DeFlorio et al., 2021).
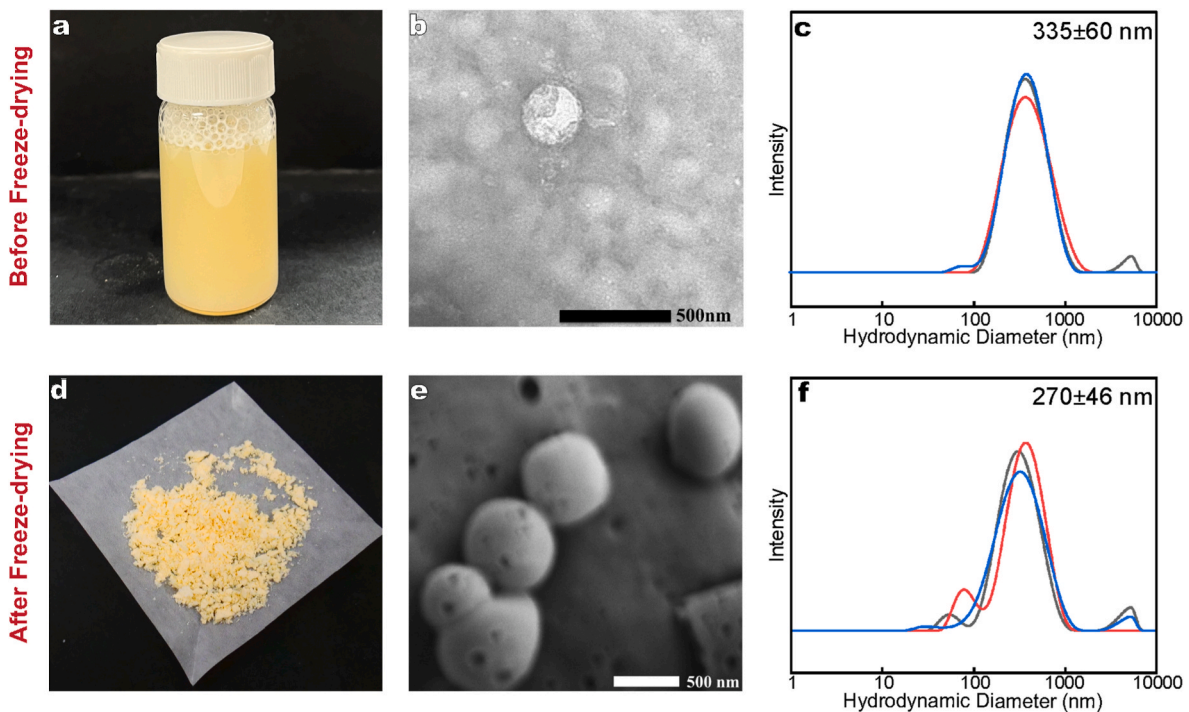
Fig. 1. The comparison of visual, morphological, and size characteristics of nano-encapsulates involving cinnamon-bark oil and whey protein before and after freeze-drying: Digital images of **(a)** nano-encapsulate suspension and **(b)** freeze-dried nano-encapsulated powder, **(c)** A TEM micrograph showing spherical morphology of nanoparticles, **(d)** A SEM micrograph of freeze-dried nano-encapsulates, and the particle size/intensity distribution of the nano-encapsulate suspension **(e)** before freeze-drying and **(f)** after freeze-drying and resuspending in DI water (three replicates, shown in different line colors). (For interpretation of the references to color in this figure legend, the reader is referred to the Web version of this article.)

In addition, such information aids in predicting and analyzing the interaction and behavior of nano-encapsulates within different environments and applications, enabling the enhancement of product safety, efficacy, and quality. The colloidal suspension of nano-encapsulates, comprising cinnamon-bark essential oil and whey protein, exhibited a uniform color with yellowish hues throughout, with minimal to no visible phase separation, indicative of the successful encapsulation of essential oil within whey protein (containing both hydrophilic and hydrophobic domains) (Fig. 1a). The spherical morphology of nano-encapsulates was clearly seen from the TEM micrograph (Fig. 1b). Dynamic light scattering characterization revealed a relatively narrow particle size/intensity distribution with diameter of 335 ± 60 nm (the intensity-averaged diameter) and a polydispersity index (PDI) of 0.21 ± 0.01 (Fig. 1c).

Considering the aqueous nature of the nano-encapsulate suspension and the lipophilic characteristic of paraffin wax, water elimination from the freshly prepared nano-encapsulate suspension is imperative. This objective was accomplished through freeze-drying, enabling the effective integration of nano-encapsulates and wax. Consequently, the freeze-dried nano-encapsulates were also extensively investigated (Fig. 1d). It was found that the nano-encapsulates retained their structural integrity and shape even after freeze-drying process (Fig. 1e). In light scattering studies, to ensure a direct comparison, the freeze-dried nano-encapsulates were resuspended in water. The particle size characteristics indicated a minor shift to a particle size of 270 ± 46 nm (the intensity-averaged diameter) and a PDI of 0.18 ± 0.01 (Fig. 1f). To gain insight into the surface charge and dissociate state of whey protein nanocarriers before and after freeze-drying, the zeta (ζ) potential of the nano-encapsulates was characterized. The ζ-potential was found to be −20.7 ± 0.13 mV and −19.7 ± 0.41 mV for samples before and after freeze-drying, respectively, indicating a statistically insignificant difference in values of the ζ-potential before and after freeze-drying ($p > 0.05$). The zeta potential of whey protein nanocarriers is negative primarily because of the ionizable amino acid residues (such as leucine and

glutamic acid) on its surface (et al., 2021; Hamarsland et al., 2017). Their carboxyl terminal groups tend to dissociate in water, releasing protons and giving rise to the whey protein surface with a net negative charge (Ravindran et al., 2018). Also, the ζ-potential values obtained agree with the literature that used the same encapsulant (Bae et al., 2022).

To chemically affirm the encapsulation of CEO within the whey protein matrix, ATR-FTIR analysis was conducted on CEO, whey protein concentrates, and freeze-dried EO-NE powders. Upon examination of the spectrogram (Supplementary Material Fig. S1) within the wave number range of 1600 cm^{-1} to 1800 cm^{-1} (IR fingerprint range for cinnamon), a prominent peak at 1639 cm^{-1} was observed. This peak corresponds to the C=O stretching characteristic of aldehydes present, notably cinnamaldehyde, the major compound in cinnamon essential oil (Y. Q. Li et al., 2013).

Analysis of the ATR-FTIR spectra of whey protein (blue curve in Fig. S1) revealed two distinct peaks of relatively equal intensity at 1535 cm^{-1} and 1640 cm^{-1}. These peaks correspond to the Amide I (C–N stretching and N–H bending) and Amide II (C=O stretching and C–N bending) vibrations, respectively (Andrade et al., 2019). Notably, the sharp peak at 1535 cm^{-1} observed in the whey protein spectrogram was absent in the FTIR spectra of CEO.

Moreover, in the ATR-FTIR spectra of EO-NE powders, an overlap between the C=O vibrational stretching peak at 1639 cm^{-1} and the characteristic Amide I peak at 1640 cm^{-1} was observed. The discrepancy in relative intensities between the peaks at 1535 cm^{-1} and 1640 cm^{-1} in the EO-NE spectra is due to this reason.

3.3. Encapsulation efficiency and percent recovery of cinnamon essential oil

Encapsulation efficiency (EE) is crucial as it directly influences the delivery and release of the encapsulated active agents, impacting the antibacterial efficacy and stability of formulations. Encapsulation
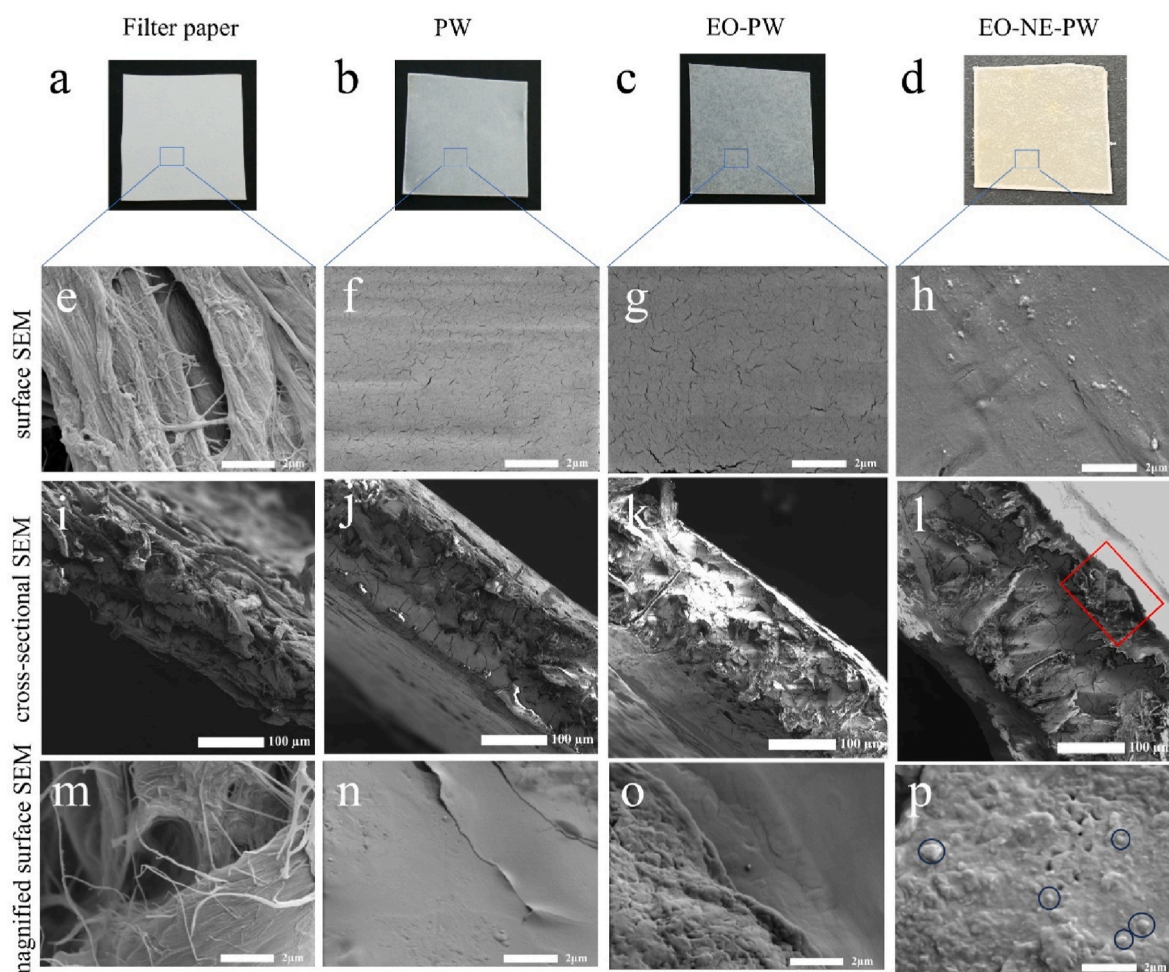
Fig. 2. (a–d) Digital images of specimens cut into square coupons of 1 cm^2 in area with their corresponding surface (**e–h**), cross-sectional (**i–l**) SEM micrographs and magnified surface SEM micrographs (**m–p**). PW indicates paraffin wax, EO-PW indicates paraffin wax mixed with essential oils, and EO-NE-PW indicates paraffin wax mixed with nanoencapsulated essential oil.

efficiency was ascertained utilizing UV–Visible spectroscopy at a wavelength of 294 nm (see supplementary material, Fig. S2). The analysis was conducted based on our calibration data for CEO, which was fitted with an equation in accordance with the Beer-Lambert Law to yield:

$$A = (2654 \pm 238.8) \times c \pm 0.1 \tag{2}$$

By employing equations 1a and 1b, the EE was determined to be 75 $\pm$ 2.9%. On the other hand, the percentage recovery was found to be 49 $\pm$ 3.5%. About 25% reduction in encapsulated CEO could be due to leakage of a portion of the CEO due to the rupture of some of the whey

protein encapsulating matrices. This could be observed by the cavity-like structures in the SEM images of the freeze-dried nano-encapsulates (shown in Fig. 1e). This decrease in the encapsulated CEO encapsulation might also be an influential factor in the reduction in nanoparticle size, shown in DLS data presented in Fig. 1f.

3.4. Surface characteristics and wetting parameters of the wax coatings

The nano structural characteristics were analyzed because they are fundamental to optimizing the formulation for enhanced performance, ensuring the homogeneity and stability of the composite system, and
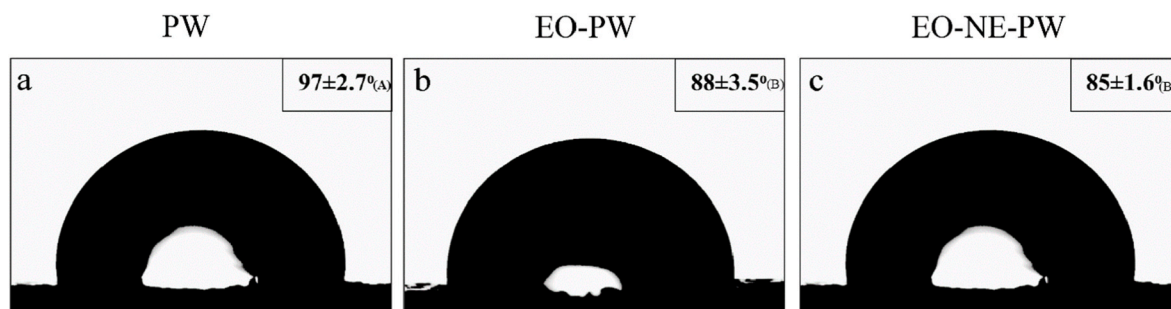
Fig. 3. Static water contact angles measured on the wax coated substrates. The letters A, B show the statistical significance obtained by performing one-way ANOVA (p = 0.05).

modulating the sustained release profiles of CEO. To this end, regular and cross-section SEM was utilized (Fig. 2). Notably, spherical features were identified in the EO-NE-PW substrates that were absent in the other three substrates (pristine filter paper, PW and, EO-PW), evident from both surface and cross-sectional SEM images (depicted in Fig. 2h and l [highlighted by red rectangular block]). To further elucidate the appearance of nanoparticles in the EO-NE-PW substrates magnified cross-sectional SEM images were captured (shown in Fig. 2p [circled in blue]). This observation highlights that most nanoparticles maintained their structural integrity within the wax matrix.

Additionally, to gain insights into the extent of dispersion of the EO-NE particles, elemental mapping using energy dispersive EDX was executed on PW and EO-NE-PW substrates, targeting carbon (C), nitrogen (N), and sulfur (S) as key elements (shown in Supplementary Material Fig. S3). The outcomes showed that there was a 0.2% enhancement in sulfur content across the substrate, with whey protein being the predominant source of sulfur (Cox et al., 2021; Lai et al., 2022) (comparing the table embedded in the Supplementary Material Fig. S3b &d). This outcome substantiated that vigorous agitation of the wax melts during the incorporation of EO-NE particles led to the homogeneous distribution of nanoparticles on the substrates.

Furthermore, a comparative analysis of the wetting behaviors of PW, EO-PW, and EO-NE-PW was conducted. The contact angle exhibited by PW measured $97 \pm 2.7°$ (shown in Fig. 3a). This value aligns consistently with previous reports on paraffin wax-based coatings (Mujika Garai et al., 2005). Moreover, it's noteworthy that a significant number of natural waxes follow to the Wenzel wetting model, resulting in complete surface wetting attributable to their relatively smooth topographies and contact angles ranging between 90 and 100° (Papadopoulos et al., 2013; Varughese and Bhandaru, 2020). Observations revealed that the contact angles on EO-PW and EO-NE-PW substrates demonstrated values of $88 \pm 3.5°$ and $85 \pm 1.6°$, respectively, with no statistical differences between the measured values (Fig. 3b &c).

When comparing the contact angles on PW and EO-NE-PW substrates, we observed a reduction in values by 13°. This reduction can be attributed to the dispersion of whey protein (hydrophilic encapsulating material) within the wax matrix. In addition, to understand the changes in the wetting behavior over time and to comprehend the water spreading on the coatings dynamic contact angle measurements were performed (shown in Supplementary Material Table S2). The contact angle measurements on PW substrates yielded advancing and receding contact angles of $102.0 \pm 0.5°$ and $61.0 \pm 0.6°$, respectively, resulting in a contact angle hysteresis of $41.0 \pm 0.6°$. These results are similar to the previously reported values (Gomes et al., 2013). Comparatively, when we examined EO-PW and EO-NE-PW substrates, we observed statistically significant differences in both the advancing and receding contact angles. For EO-PW, the advancing contact angle was $98.0 \pm 1.3°$, and the receding contact angle was $68.0 \pm 1.1°$, resulting in a hysteresis of $30 \pm 1.3°$. In the case of EO-NE-PW coatings, the advancing contact angle measured $90 \pm 1.1°$, while the receding contact angle was $53.0 \pm 1.6°$, resulting in a hysteresis of $37 \pm 1.6°$. Thus, in comparison to EO-PW substrates the EO-NE-PW coatings showed higher contact angle hysteresis indicating a higher degree of water spreading on the coating. This phenomenon ensures better contact between water droplets containing bacteria and the embedded antibacterial bioactive compounds (CEO), thereby amplifying their efficacy. Furthermore, the static contact angles exhibited by EO-NE-PW coatings were found to be analogous to the contact angles observed on natural apple waxes (Hall, 1966).

Within the fruit processing industries, a prevalent practice involves the application of artificial cuticular waxes through the dip coating technique, followed by refinement using wax polishing brushes and rollers (Ruiz-Llacsahuanga et al., 2022; Sanchez-Tamayo et al., 2024). These polishing methods introduce additional variables, including alterations in surface roughness, wetting properties, and the potential disruption of certain infused EO-NE nanoparticles closer to the surface. These factors are subject to variation. In the context of this manuscript,
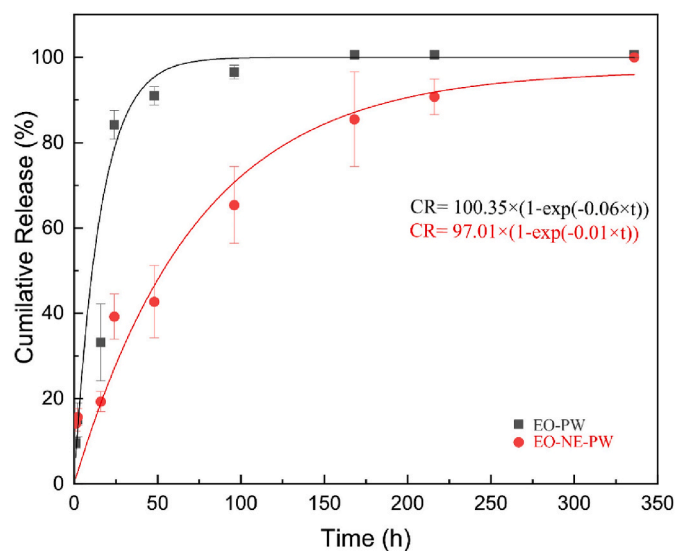
Fig. 4. Release kinetics of embedded cinnamon-bark essential oil through the dialysis pouch. Comparison of release through paraffin wax substrates with their corresponding fitting lines.

we intend to discuss the characteristics of the coatings as prepared to have a universal comparison.

3.5. Release kinetics of cinnamon essential oil

To assess the advantages of infusing encapsulated CEO as opposed to merely dispersing CEO within paraffin wax, a release kinetics study was conducted. This study aimed to evaluate the extent of slow and sustained release of CEO. From a standpoint of relevance, it is critical to acknowledge that in the food processing industries, a significant proportion of bacterial contaminants on surfaces stem from waterborne sources (Gallo et al., 2020). Consequently, water serves as the primary medium through which bacteria contact surfaces playing a critical role in the transmission of bacteria. Hence, understanding the release dynamics of the active ingredient, in this instance, CEO, in aqueous medium becomes relevant.

The release kinetics investigation spanned a duration of 336 h, equivalent to 14 days. It was observed that, well before the conclusion of this 14-day period, each specimen exhibited plateauing of the CEO release profile. To facilitate a comparative analysis, each release profile was appropriately normalized (with reference to the 14-day release duration). It is important to note that our study did not allow for the complete 100% release of CEO from the paraffin wax into the bulk DI water solution. Several factors contributed to this incomplete release, including the preferential adhesion of CEO to the paraffin wax due to hydrophobic interactions and the absorption of some CEO into the filter paper substrates during the coating procedures. Our study was designed with a primary objective of comparing the release behavior of CEO in the context of encapsulation versus the conventional approach of utilizing CEO in commercial wax coatings, where it is typically dispersed in bulk within the paraffin matrix (Kouassi et al., 2012; Orafidiya et al., 2001). Therefore, a quantitative assessment of the extent of CEO adsorption to the paraffin wax, as well as the portion that remains within the paraffin wax due to stronger hydrophobic interactions, is a topic of investigation in our further studies.

The release kinetics study, conducted by dispersing EO-NE particles within a dialysis membrane submerged in DI water, is presented in Supplementary Material Fig. S4 and release kinetics study through EO-PW and EO-NE-PW substrates is shown in Fig. 4. The outcomes of the fitting and the interpretation of each of the terms obtained from the utilized fitting equation are described in Supplementary Material
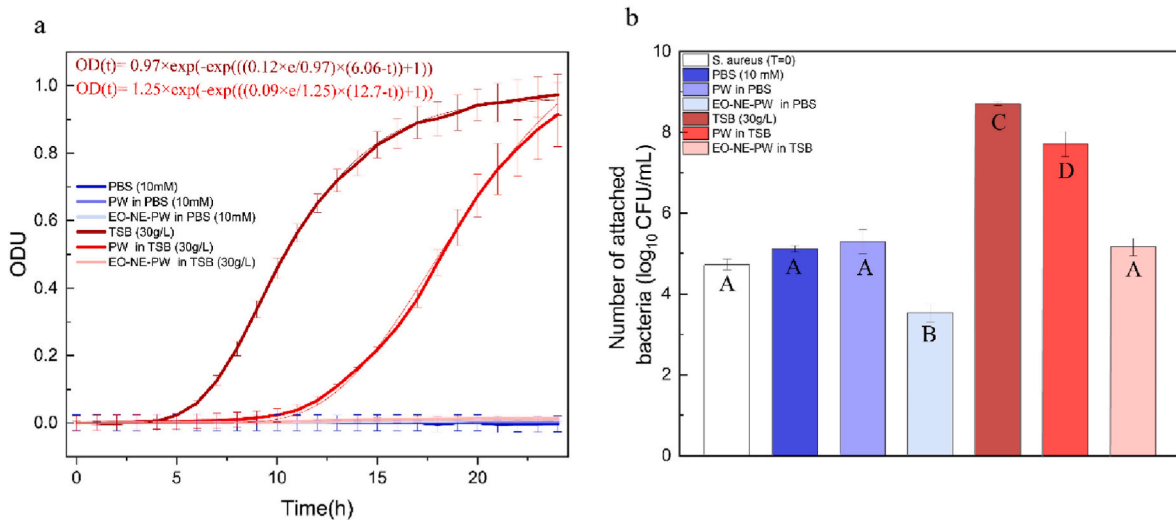
Fig. 5. a. Graphical representation of kinetic growth studies of *Staphylococcus aureus* (using OD measurements) with the re-parametrized Gompertz fitting lines shown by lines of thickness 0.5. **b.** Bacterial enumerations (in the media) calculated before (t = 0 h) and after (t = 24 h) the OD experiment on each of the specimen. The letters (A–D) represent statistical analysis with a significance level set at p = 0.05.

Table S3.

Notably, our observations revealed a significant difference in the half-lives: the time required for 50% of the releasable CEO, calculated through first-order kinetic fitting of release profiles for the EO-NE, EO-PW, and EO-NE-PW specimens. The calculated mean half-life values for these specimens were found to be 5.34 h, 11.49 h, and 72.45 h, respectively.

These findings illuminate a significant observation. The encapsulation of CEO using whey protein has the potential to extend the half-life by approximately 61 h when compared to non-encapsulated counterparts, ensuring a slow and sustained release of the bioactive compounds. Additionally, the whey protein, which has been proven to be an effective odor-masking agent, prevents the strong smells encountered by consumers (through their application on fruits) facilitated by delayed release (S. Yang et al., 2012).

3.6. Influence of essential oil-based nanoparticle-embedded hybrid wax coatings on bacterial growth

In the context of the fruit and vegetable processing industries, bacterial contamination and cross-contamination arises from a multitude of factors, including non-hygienic operational practices, human intervention, and insufficient sanitization measures (Balali et al., 2020; Kouassi et al., 2012). To avert such an undesirable scenario, it becomes important for coatings to suppress bacterial growth.

To comprehend the growth kinetics of the gram-positive and gram-negative bacterial organisms when exposed to PW and EO-NE-PW substrates, OD measurements in growth media were conducted. To gain a deeper understanding of the insights derived from the OD curves, a three-parameter sigmoidal fitting approach was employed, involving the re-parametrized Gompertz model (Carrascosa et al., 2021; Lo Grasso et al., 2023). Generalized equations and descriptions of the model parameters along with the terms obtained post fitting can be found in the Supplementary Material Table S4.

When the growth of *S. aureus* in TSB was compared with its growth in
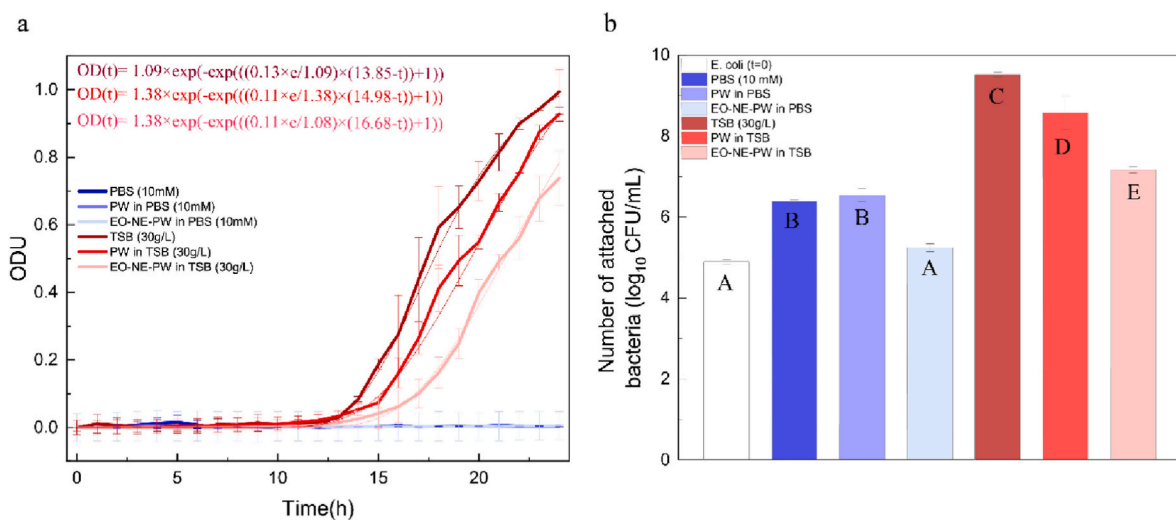
Fig. 6. a. Graphical representation of kinetic growth studies of *Escherichia coli* O157:H7 (using OD measurements) with the re-parametrized Gompertz fitting lines (shown by corresponding lines with thickness of 0.5) and equations. **b.** *E. coli* enumerations calculated before (t = 0 h) and after (t = 24 h) the OD experiment on each of the specimen. The letters (A–E) indicate the statistical significance (p = 0.05).
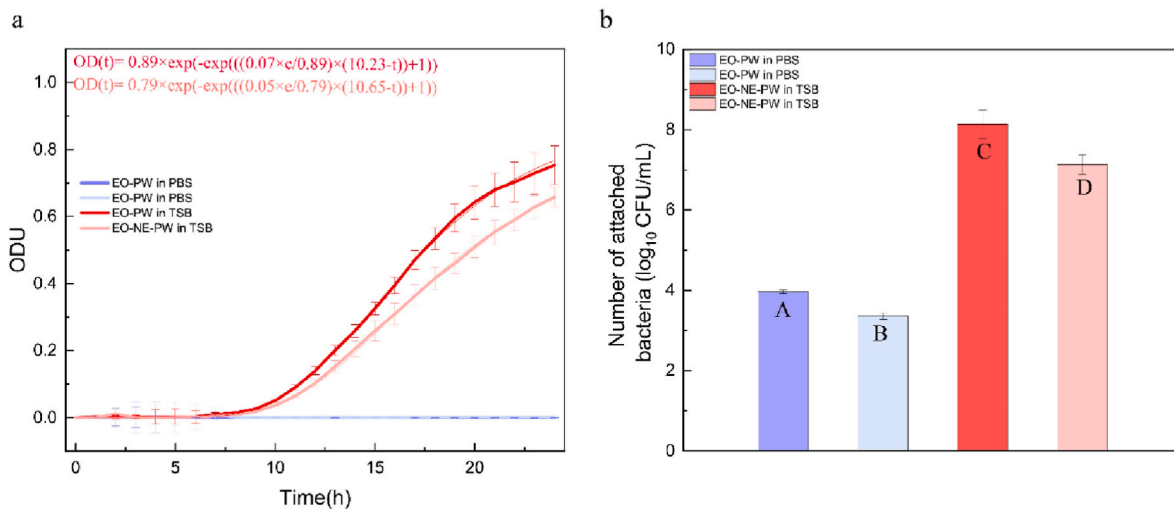
Fig. 7. a. Kinetic growth studies of *Staphylococcus aureus* (72 h after essential oil release in DI water) with fitting lines (marked by line thickness 0.5) and corresponding equations, and **b.** Its enumerations after 24 h of the OD experiment, where letters A-D indicate statistical distinctions (at p = 0.05).

the presence of PW substrates (Fig. 5a), a significant increase in the lag time (λ) was observed, extending from 6.06 ± 0.02 h to 12.74 ± 0.01 h. Furthermore, a reduction in the maximum specific growth-rate (μ_m) was evident, transitioning from 0.12 ± 0.01 in the case of the control *S. aureus* inoculum to 0.09 ± 0.01 in the presence of PW substrates (Supplementary Material Table S4). These phenomena appear attributable to the adhesion of certain bacterial colonies onto the paraffin wax coatings and cannot be recorded by the spectrophotometer. The mechanism underlying this bacterial adhesion can be primarily ascribed to hydrophobic-hydrophobic interactions between the bacterial cell wall and the substrate (Grimaud, 2010). Enhanced adhesion is also likely facilitated by the release of extracellular binding substances (EBS) (Oh et al., 2018). Importantly, it is worth mentioning that no discernible alteration in optical density was observed in *S. aureus* suspensions in PBS (10 mM) solutions that were exposed to PW and EO-NE-PW substrates, as well as when *S. aureus* cultures at the same concentrations suspended in TSB exposed to EO-NE-PW substrates. The release of the CEO from the EO-NE-PW substrates has proven to be successful in inhibiting the growth of *S. aureus*, even in highly growth-promoting media like TSB. To obtain the exact populations of bacteria in the well plates, quantification was performed.

Initial enumeration (t = 0 h) of *S. aureus* suspensions subjected to a 1000-fold dilution revealed a population of 4.7 ± 0.13 $\log_{10}$ CFU/mL. Following a 24-h incubation period at a temperature of 25 °C, bacterial enumeration was carried out. The bacterial populations exhibited a slight increase in PBS (10 mM), recording values of 5.1 ± 0.08 $\log_{10}$ CFU/mL (statistically insignificant p > 0.05), while a more pronounced elevation was observed in TSB, reaching 8.7 ± 0.04 $\log_{10}$ CFU/mL. In the presence of PW, bacterial counts exhibited values of 5.3 ± 0.30 $\log_{10}$ CFU/mL in PBS and 7.7 ± 0.31 $\log_{10}$ CFU/mL in TSB, respectively. Similarly, in EO-NE-PW, *S. aureus* counts averaged 3.5 ± 0.23 $\log_{10}$ CFU/mL in PBS and 5.2 ± 0.22 $\log_{10}$ CFU/mL in TSB (Fig. 5b).

When comparing the growth curves of *E. coli*, the fitting of the OD data revealed λ values of 13.85 ± 0.07, 14.98 ± 0.13, and 16.68 ± 1.25 h for the control inoculum, PW, and EO-NE-PW in TSB, respectively (Fig. 6a, with values shown in Supplementary Material Table S4). A 1.5 h delay in the bacterial growth (lag phase) in the presence of EO-NE-PW substrates in comparison to the PW substrates shows the anti-bacterial effect of the released CEO into the growth media.

Similar to the enumeration outcomes attained for *S. aureus*, a mean count of 4.9 ± 0.05 $\log_{10}$ CFU/mL was obtained following the 1000-fold dilution of the second transfers of *E. coli* suspensions. Following an incubation of 24 h at 25 °C, a substantial increase in *E. coli* numbers was

evident both in PBS and TSB: 6.4 ± 0.05 and 9.5 ± 0.05 $\log_{10}$ CFU/mL, respectively. In the presence of PW, the enumeration of *E. coli* produced means of 6.5 ± 0.16 $\log_{10}$ CFU/mL in PBS and 8.6 ± 0.42 $\log_{10}$ CFU/mL in TSB. Similarly, when EO-NE-PW was introduced, bacterial enumeration yielded 5.3 ± 0.09 $\log_{10}$ CFU/mL in PBS and 7.2 ± 0.08 $\log_{10}$ CFU/mL in TSB media (refer Fig. 6b).

Following a 24-h exposure period of the contaminated solutions in PBS and TSB, a discernible reduction in the *S. aureus* bacterial populations was observed, measuring at 1.8 ± 0.4 $\log_{10}$ CFU/mL and 3.5 ± 0.3 $\log_{10}$ CFU/mL, respectively. Similarly, the *E. coli* bacterial populations demonstrated a decrease, with values of 1.2 ± 0.2 $\log_{10}$ CFU/mL in PBS and 1.4 ± 0.4 $\log_{10}$ CFU/mL in TSB. In comparison to the control inocula, the lag times were notably higher in the presence of PW substrates for *S. aureus* as compared to the *E. coli*. This phenomenon could be attributed to the enhanced adhesion of macromolecules on the surface of the cell wall of *S. aureus* to the wax coatings (binding interactions). These interactions play a crucial role not only in the primary adhesion phase but also in subsequent processes of biofilm formation (Maikranz et al., 2020).

In alignment with established literature, it is noteworthy that *E. coli* exhibited heightened resilience to dissolved CEO compared to *S. aureus* (Byung Hong Kim, 2008; Clemente et al., 2016; Ju et al., 2023). This discrepancy can be ascribed to inherent structural disparities between the bacterial species. Specifically, owing to the presence of an outer membrane, *E. coli* demonstrates augmented resistance against the adverse effects induced by CEO. This support arises from the obstructive nature of the outer membrane, which hinders the passage of hydrophobic components. The lipopolysaccharides present in the gram-negative bacteria provide resistance against the hydrophobic compounds attempting to enter the bacteria (Byung Hong Kim, 2008).

3.7. Superiority of encapsulated-essential oil dispersion in wax coatings

To assess the sustained antibacterial effect achieved by dispersing EO-NE particles within the paraffin wax matrix, an endurance evaluation of the coatings was conducted. EO-PW and EO-NE-PW strips were immersed in DI water for 72 h, which corresponds to the half-life of EO-NE-PW coatings before the bacterial growth was monitored using OD measurements.

Non-linear fitting of the OD values was performed using the Gompertz model (shown in Fig. 7a). The analysis revealed λ values of 10.23 ± 0.04 and 10.65 ± 0.06 h for the growth of *S. aureus* in the presence of EO-PW and EO-NE-PW substrates, respectively, in TSB growth media
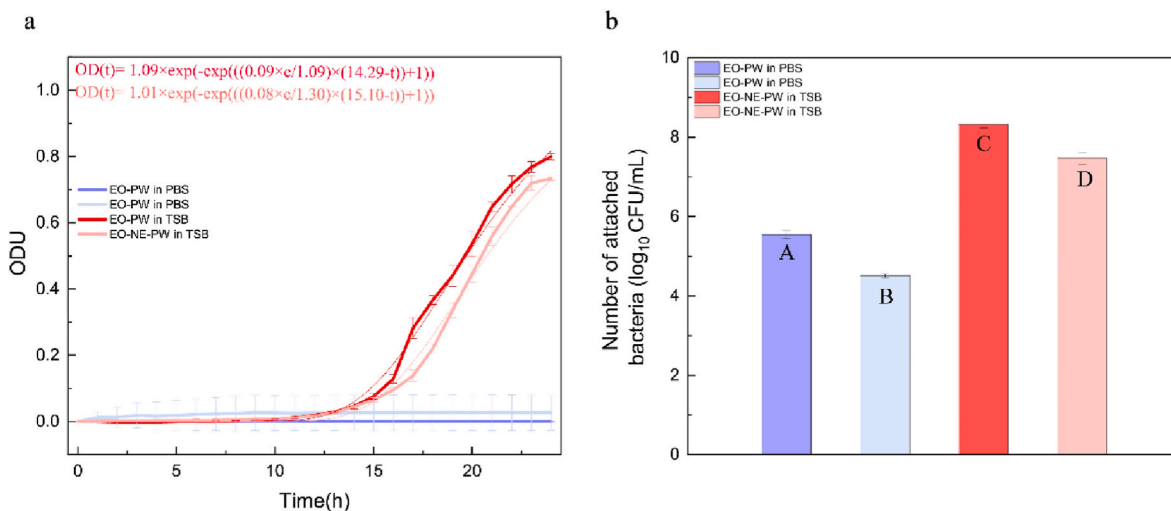
Fig. 8. a. Kinetic growth studies of *Escherichia coli* (72 h after essential oil release in DI water) with fitting lines (marked by line thickness 0.5), and corresponding enumerations after 24 h of the OD experiment, where letters A-D indicate statistical distinctions (at p = 0.05).

(shown in Supplementary Material Table S4) and no discernible change in the OD values in PBS media in the presence of the two coated substrates. Similarly, the maximum achievable OD value (A) decreased from 0.89 ± 0.02 to 0.79 ± 0.01 when transitioning from EO-PW to EO-NE-PW substrates. This extension of the lag phase and reduction in the maximum achievable OD values demonstrate the significant antibacterial activity of EO-NE-PW over EO-PW substrates (post three-day release in DI water) primarily attributable to encapsulation.

In addition, the logarithmic-scale enumeration of *S. aureus* inoculums from well plates after completion of the OD measurements (t = 24 h) revealed populations of 4.0 ± 0.05 and $3.4 \pm 0.08 \log_{10}$ CFU/mL in PBS media in the presence of EO-PW and EO-NE-PW respectively and in TSB growth media the populations were calculated to be 8.14 ± 0.35 and $7.13 \pm 0.25 \log_{10}$ CFU/mL when contacted with EO-PW and EO-NE-PW substrates respectively (shown in Fig. 7b). Hence, a statistically significant (p < 0.05) difference in the log-scale *S. aureus* population (a reduction of $0.6 \pm 0.08 \log_{10}$ CFU/mL in PBS and $1.01 \pm 0.35 \log_{10}$ CFU/mL in TSB) underscores the importance of employing nano-encapsulated essential oil particles within the wax matrix.

After fitting the growth curves of *E. coli* (in TSB), the λ values in the presence of EO-PW and EO-NE-PW substrates were obtained as 14.29 ± 0.13 and 15.10 ± 1.67 h respectively while, the 'A' values were 1.09 ± 0.08 and 1.00 ± 0.64 respectively while the growth was flat-lined in PBS media. As mentioned earlier, the extension of the lag phase was also observed in the case of *E. coli* growth which marks the pronounced antibacterial after even after 72-h release (attributable to encapsulation).

It is interesting to note that the lag phase for the growth of *E. coli* in TSB in the presence of EO-NE-PW which was 16.68 ± 1.25 h in our previous assay (monitoring bacterial growth in TSB immediately after samples were prepared) decreased to 15.10 ± 1.67 h when growth was monitored following immersion into DI water for 72 h (refer Supplementary Material Table S4). This further substantiates the plateauing nature of the release of CEO (decreasing rate of CEO release) through EO-NE-PW.

The log-scale bacterial populations (of *E. coli*) were evaluated as 5.5 ± 0.09 and $4.5 \pm 0.04 \log_{10}$ CFU/mL in PBS media and of 8.32 ± 0.08 and $7.46 \pm 0.14 \log_{10}$ CFU/mL in TSB growth media when the bacterial cultures were contacted with EO-PW and EO-NE-PW respectively (shown in Fig. 8b). Therefore, encapsulation of essential oil signified (p < 0.05) the difference in the number of viable bacterial colonies (*E. coli*), demonstrating reductions of $1.00 \pm 0.10 \log_{10}$ CFU/mL and $0.90 \pm 0.10 \log_{10}$ CFU/mL in PBS and TSB media respectively compared to its un-
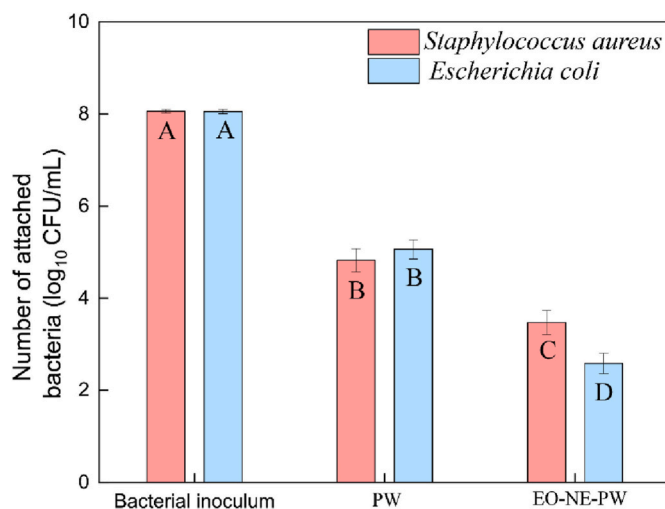
Fig. 9. Enumeration of bacterial populations on the two wax coated substrates in comparison to the control inoculums. The letters (A–D) represent statistical distinction (p = 0.05) between the values.

encapsulated counterparts.

Thus, controlled bacterial growth in a growth media, combined with a substantial reduction in the bacterial population when exposed to EO-NE-PW substrates compared to EO-PW substrates, demonstrates the advantages of utilizing nano-encapsulated particles in wax formulations. This is particularly advantageous for fruits with extended storage times that undergo transportation to other countries, often involving shipping durations of 3–5 days.

3.8. Shaker plate assay

To emulate waterborne cross-contamination on the wax coatings of fruits, we designed a shaker plate assay to quantify the transfer of bacteria from bacteria-laden DI water to the wax-coated substrate. This assay is relevant from an industrial standpoint as cross-contamination resulting from unhygienic food contact surfaces, inadequate sanitization of harvested fruits and vegetables, and potential contamination during handling by animals and humans is common in the food processing industries (Carrasco et al., 2012; Stand, 2020). It is of high significance for the novel technologies to not only suppress bacterial
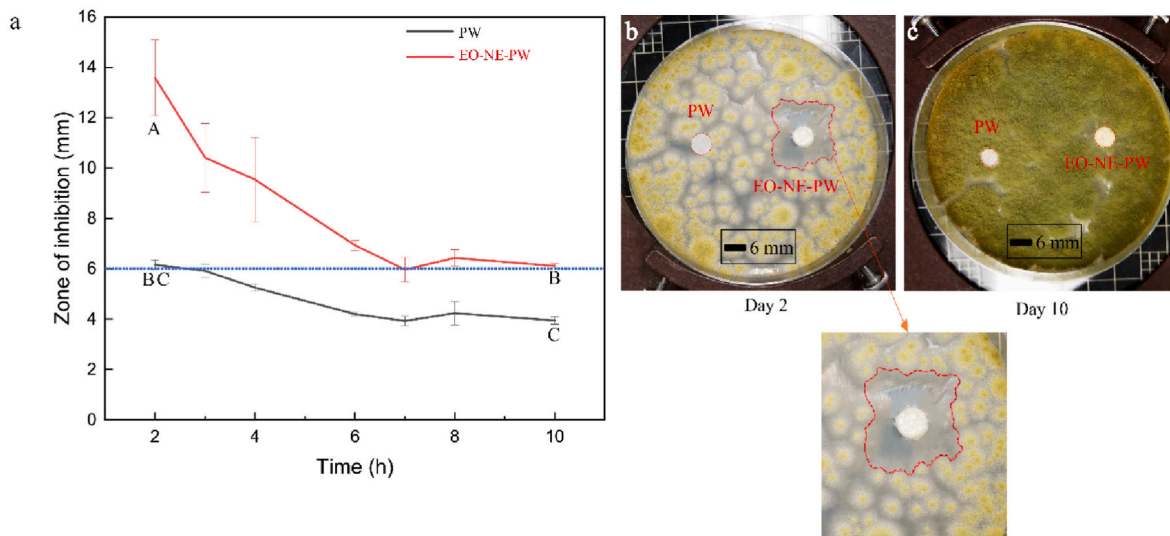
Fig. 10. a. Graphical representation of zone of inhibitions in the presence of the wax substrates in *Aspergillus flavus* mycelium. **(b, c).** Images of agar plates (with circular discs of coated substrates) after **b.** 2-Day and **c.** 10-day of incubation at 37 °C.

growth but also decrease their adhesion during these relatively brief contact intervals. 10-fold dilutions of second transfer-suspensions, dispersed in DI water, were exposed to filter papers with equal surface areas coated with PW and EO-NE-PW. After a 1-h exposure to bacterial inoculum, observations revealed the level of bacterial transfer onto PW substrates averaged 4.8 ± 0.25 log$_{10}$ CFU/mL for *S. aureus* and 5.1 ± 0.21 log$_{10}$ CFU/mL for *E. coli*. Similarly, bacterial transfer onto EO-NE-PW substrates was found to be 3.5 ± 0.26 log$_{10}$ CFU/mL for *S. aureus* and 2.6 ± 0.22 log$_{10}$ CFU/mL for *E. coli* (Fig. 9).

Interaction among planktonic bacteria and their interactions with surfaces is studied using Derjaguin Landau-Verwey-Overbeek interactive theory (Y. Cheng et al., 2019; DeFlorio et al., 2023; Hermansson, 1999). In short, the interaction between the colloidal particles (planktonic bacterium in our case) and the hydrophobic wax substrates is governed by two vital components, namely van der Waals attractions and repulsions due to the formation of electrostatic double layer around the negatively charged bacteria. There was a significant difference in the bacterial adhesion to the two wax substrates for both *S. aureus* and *E. coli*. This distinction is observed even though EO-NE-PW substrates (compared to the PW substrates) exhibit higher water wetting characteristics (indicated by lower contact angles, as shown in Fig. 3c), which leads to increased proximity of the bacteria to the substrates, where van der Waals attractions emerge as the dominant mode of interaction between the bacteria and the wax coatings.

This phenomenon of 1.3 ± 0.2 log$_{10}$ CFU/mL and 2.5 ± 0.3 log$_{10}$ CFU/mL reduction in bacteria populations of *S. aureus* and *E. coli* adhering on to the EO-NE-PW substrates in comparison to PW substrates is due to the timely release of bioactive compounds from the EO-NE-PW substrates that prevent the bacteria to adhere to the EO-NE-PW substrates. Furthermore, the notable statistically significant difference in the populations of *E. coli* and *S. aureus* on EO-NE-PW substrates can be explained by considering the elevated electrostatic repulsions between *S. aureus* (with a ζ potential of -39 ± 0.17 mV) and the hydroxyl and carbonyl functional groups present in the paraffin wax. This contrast is evident when compared to the ζ potential of *E. coli*, which is marginally lower (in magnitude) at -30 ± 1.9 mV.

3.9. Growth inhibition of fungus by cinnamon essential oil embedded wax substrates: disc diffusion assay

During the marketing of fruits, extended periods of storage within warehouses often occur, either as they await sale or during export to other countries. In certain instances, the storage conditions, encompassing humidity, temperature, and ambient contaminants, can provide a favorable environment for the proliferation of fungi (Barkai-golan, 2007; Yadav and Heitman, 2022). Furthermore, fruits affected with fungi are prone to foodborne pathogens when they have pre-residing fungal spores on them (Graça et al., 2017). Therefore, it is crucial for the innovative fruit coatings to effectively prevent fungal growth.

For the comparative analysis of inhibitory effects resulting from fungal contaminations on both EO-NE-PW and PW substrates, the Kirby-Bauer assay was employed, and the pre-sterilized samples (in the agar) were monitored for fungal growth over a 10-day period. For this assay we use *A. flavus*, one of the common species in the saprophytic filamentous fungal genus *Aspergillus* known to cause black molds in red apples (Alegbeleye et al., 2022; Hatmaker et al., 2022; Keykhosravi, 2018). It is an accepted phenomenon that the clear zone (zone of inhibition) formed around the filter paper is attributable to the presence of antifungal materials within the filter paper. The diffusion of CEO through the agar to observe distinct inhibition zones required 48 h (2 days) of incubation. Following this, the zone of inhibition surrounding EO-NE-PW substrates measured 13.5 ± 0.15 mm, whereas for PW substrates, it was 6.2 ± 0.18 mm, indicating an absence of inhibition around the circular wax pellet. Subsequently, under incubatory conditions at 37 °C, the agar plates were observed over a 10-day period. By the third day, a few strands of hyphae and conidiophores commenced extending onto the PW substrates. In contrast, no such phenomenon was evident on the EO-NE-PW substrates, even upon reaching the 10-day incubation period (Fig. 10c). To detect the statistical differences in sizes of the observed zone of inhibitions as indicative of an antifungal effect of treatment, a one-way ANOVA was conducted for mean zone diameters for data from 2 to 10 days of incubation. A clear distinction was observed in the zone of inhibitions calculated after 2-day and 10-day incubation of the inoculated agar plates (represented by letters A, B, C in Fig. 10a).

3.10. Visual appearance of hybrid wax coatings on produce

In addition to extending shelf life through superior antimicrobial properties, it is essential that fruit coatings also possess cosmetic appeal to attract consumers (Lv et al., 2022; Massaglia et al., 2019; Rahman et al., 2021). Recent research has reported a direct correlation between fruit attractiveness, consumer preference, and overall profitability (Wang et al., 2022; Wunsch, 2023). Furthermore, in the context of
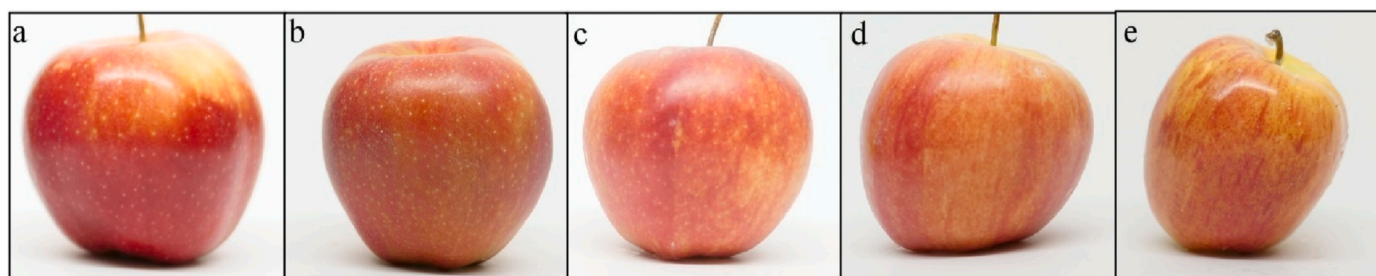
Fig. 11. Digital images of red apples **a.** As purchased from local grocery store **b.** After washing with chloroform to remove the natural and applied wax (in the processing industry) **c.** Coated with paraffin wax, **d.** Coated with cinnamon essential oil dispersed wax formulations **e.** Coated with freeze dried cinnamon essential oil nanoparticles dispersed paraffin wax formulations. (For interpretation of the references to color in this figure legend, the reader is referred to the Web version of this article.)

global fruit export, meeting international cosmetic standards is an important factor that empowers producers to secure higher returns for their products, consequently enhancing the overall profitability of fruit production (Bhat et al., 2015; S. H. Yang and Panjaitan, 2021).

In the pursuit of evaluating the cosmetic impact of different coatings on red apples, including pristine wax, CEO-dispersed wax, and EO-NE particles in wax (shown in Fig. 11), an observational study was conducted. To assess the visual attributes of these coated apples, apples sourced from local grocery stores, initially treated with wax during fruit processing, were subjected to a chloroform washing process to eliminate the existing wax coating. It was observed when the wax from the surface of the apples was removed, the fruits looked dull and devoid of luster (shown in Fig. 11b). Remarkably, the results revealed no discernible differences in the appearance of apples treated with these three distinct wax formulations: pristine wax, CEO-dispersed wax, and EO-NE particles in wax (as illustrated in Fig. 11a–c, d).

4. Conclusion

In this comprehensive investigation, we have pioneered the development of novel nanoparticle-infused wax coatings suitable for application on red apples. The rate of release of CEO substantially decreased, resulting in a 61-h delay in achieving a 50% release of the embedded bioactive compounds compared to non-encapsulated coatings.

The novel coatings produced a significant reduction in viable bacterial counts in PSB and TSB compared to controls coated with paraffin wax after 24 h of exposure, with reductions of 1.8 ± 0.4 $\log_{10}$ CFU/mL (PBS) and 3.5 ± 0.3 $\log_{10}$ CFU/mL (TSB) for *S. aureus*, and 1.2 ± 0.2 $\log_{10}$ CFU/mL (PBS) and 1.4 ± 0.4 $\log_{10}$ CFU/mL (TSB) for *E. coli*. The anti-bacterial effect of the coatings was prevalent even after 72 h immersion in aqueous media followed by bacterial exposure providing log-scale reductions of 0.6 ± 0.08 $\log_{10}$ CFU/mL (PBS) and 1.01 ± 0.35 $\log_{10}$ CFU/mL (TSB) for *S. aureus*, and 1.0 ± 0.10 $\log_{10}$ CFU/mL (PBS) and 0.9 ± 0.10 $\log_{10}$ CFU/mL (TSB) for *E. coli* in comparison to their unencapsulated wax formulation counterparts. Furthermore, our novel coatings exhibited significantly reduced bacterial attachment compared to pristine wax-coated substrates. The coatings also showed a great aversion toward *A. flavus* with the initial zone of inhibition measuring 13.5 ± 0.15 mm and no hyphae and conidiophores growth on the substrates (with coatings) even after 10 days. Herein, we have developed an innovative hybrid edible wax coating formulation with potential application on red apples. Our focus was on investigating its prolonged anti-bacterial and anti-fungal properties, achieved through the sustained release of nano encapsulated cinnamon essential oil. Notably, these coatings also effectively preserved the apples' aesthetic appeal and visual allure. Moving forward, our future studies aim to explore the extension of shelf life by conducting comprehensive chemical and physical analyses, along with sensory evaluations, of the red apples treated with our wax formulations.

CRediT authorship contribution statement

Yashwanth Arcot: Conceptualization, Methodology, Formal analysis, Investigation, Writing – original draft. **Minchen Mu:** Formal analysis, Investigation. **Yu-Ting Lin:** Investigation. **William DeFlorio:** Methodology, Resources. **Haris Jebrini:** Methodology, Resources. **Angela Parry-Hanson Kunadu:** Methodology, Investigation, Resources. **Yagmur Yegin:** Conceptualization, Resources. **Younjin Min:** Methodology, Resources. **Alejandro Castillo:** Methodology, Resources. **Luis Cisneros-Zevallos:** Supervision, Methodology, Funding acquisition. **Thomas M. Taylor:** Supervision, Methodology, Resources, Writing – review & editing. **Mustafa E.S. Akbulut:** Supervision, Conceptualization, Methodology, Resources, Funding acquisition, Writing – review & editing.

Declaration of competing interest

The authors declare that they have no known competing financial interests or personal relationships that could have appeared to influence the work reported in this paper.

Data availability

Data will be made available on request.

Acknowledgements

Appendix A. Supplementary data

Supplementary data to this article can be found online at https://doi.org/10.1016/j.crfs.2023.100667.

References

Adainoo, B., Thomas, A.L., Krishnaswamy, K., 2023. A comparative study of edible coatings and freshness paper on the quality of fresh North American pawpaw (Asimina triloba) fruits using TOPSIS-Shannon entropy analyses. Curr. Res. Food Sci. 7, 100541 https://doi.org/10.1016/j.crfs.2023.100541.

Aguilar-Morales, A.I., Alamri, S., Voisiat, B., Kunze, T., Lasagni, A.F., 2019. The role of the surface nano-roughness on the wettability performance of microstructured metallic surface using direct laser interference patterning. Materials 12 (7). https://doi.org/10.3390/ma12172737.

Alegbeleye, O., Odeyemi, O.A., Strateva, M., Stratev, D., 2022. Microbial spoilage of vegetables, fruits and cereals. Applied Food Research 2 (1), 100122. https://doi.org/10.1016/j.afres.2022.100122.

Ali, S.M., Khan, A.A., Ahmed, I., Musaddiq, M., Ahmed, K.S., Polasa, H., Rao, L.V., Habibullah, C.M., Sechi, L.A., Ahmed, N., 2005. Antimicrobial activities of Eugenol and Cinnamaldehyde against the human gastric pathogen Helicobacter pylori. Ann. Clin. Microbiol. Antimicrob. 4, 20. https://doi.org/10.1186/1476-0711-4-20.

Alizadeh Behbahani, B., Falah, F., Lavi Arab, F., Vasiee, M., Tabatabaee Yazdi, F., 2020. Chemical composition and antioxidant, antimicrobial, and antiproliferative activities of cinnamomum zeylanicum bark essential oil. Evidence-Based Complementary and Alternative Medicine. https://doi.org/10.1155/2020/5190603, 2020.

Andrade, J., Pereira, C.G., Almeida Junior, J. C. de, Viana, C.C.R., Neves, L.N. de O., Silva, P. H. F. da, Bell, M.J.V., Anjos, V. de C. dos, 2019. FTIR-ATR determination of protein content to evaluate whey protein concentrate adulteration. Lwt 99 (March), 166–172. https://doi.org/10.1016/j.lwt.2018.09.079, 2018.

Arcot, Y., Liu, S., Ulugun, B., DeFlorio, W., Bae, M., Salazar, K.S., Taylor, T.M., Castillo, A., Cisneros-Zevallos, L., Scholar, E.M.A., 2021. Fabrication of robust superhydrophobic coatings onto high-density polyethylene food contact surfaces for enhanced microbiological food safety. ACS Food Science and Technology 1 (7), 1180–1189. https://doi.org/10.1021/acsfoodscitech.1c00082.

Bae, M., Lewis, A., Liu, S., Arcot, Y., Lin, Y.T., Bernal, J.S., Cisneros-Zevallos, L., Akbulut, M., 2022. Novel biopesticides based on nanoencapsulation of azadirachtin with whey protein to control fall armyworm. J. Agric. Food Chem. 70 (26), 7900–7910. https://doi.org/10.1021/acs.jafc.2c01558.

Balali, G.I., Yar, D.D., Afua Dela, V.G., Adjei-Kusi, P., 2020. Microbial contamination, an increasing threat to the consumption of fresh fruits and vegetables in today's world. International Journal of Microbiology. https://doi.org/10.1155/2020/3029295, 2020.

Banu A, T., Ramani P, S., Murugan, A., 2020. Effect of seaweed coating on quality characteristics and shelf life of tomato (Lycopersicon esculentum mill). Food Sci. Hum. Wellness 9 (2), 176–183. https://doi.org/10.1016/j.fshw.2020.03.002.

Barkai-golan, r., 2007. ScienceDirect - Postharvest Diseases of Fruits and Vegetables, vol. 13, pp. 113–120. References. http://www.sciencedirect.om.hu/science?_ob=Article URL&_udi=B84, 1996.

Bashir, O., Amin, T., Hussain, S.Z., Naik, H.R., Goksen, G., Wani, A.W., Manzoor, S., Malik, A.R., Wani, F.J., Proestos, C., 2023. Development, characterization and use of rosemary essential oil loaded water-chestnut starch based nanoemulsion coatings for enhancing post-harvest quality of apples var. Golden delicious. Curr. Res. Food Sci. 7, 100570 https://doi.org/10.1016/j.crfs.2023.100570.

Bhardwaj, S., Lata, S., Garg, R., 2023. Application of nanotechnology for preventing postharvest losses of agriproducts. J. Hortic. Sci. Biotechnol. 98 (1), 31–44. https://doi.org/10.1080/14620316.2022.2091488.

Bhat, R., Geppert, J., Funken, E., Stamminger, R., 2015. Consumers perceptions and preference for strawberries—a case study from Germany. Int. J. Fruit Sci. 15 (4), 405–424. https://doi.org/10.1080/15538362.2015.1021408.

Bohinc, K., Štukelj, R., Abram, A., Jerman, I., Van de Velde, N., Vidrih, R., 2022. Biophysical characterization of autochthonous and new apple cultivar surfaces. Agronomy 12 (9), 2051. https://doi.org/10.3390/agronomy12092051.

Bouaziz, A., Dridi, D., Gargoubi, S., Zouari, A., Majdoub, H., Boudokhane, C., Bartegi, A., 2021. Study on the grafting of chitosan-essential oil microcapsules onto cellulosic fibers to obtain bio functional material. Coatings 11 (6), 637. https://doi.org/10.3390/coatings11060637.

Byung Hong Kim, G.M.G., 2008. Bacterial Physiology and Metabolism. Cambridge University Press.

Cai, L., Wu, D., Xia, J., Shi, H., Kim, H., 2019. Influence of physicochemical surface properties on the adhesion of bacteria onto four types of plastics. Sci. Total Environ. 671, 1101–1107. https://doi.org/10.1016/j.scitotenv.2019.03.434.

Carmona-Hernandez, S., Reyes-Pérez, J.J., Chiquito-Contreras, R.G., Rincon-Enriquez, G., Cerdan-Cabrera, C.R., Hernandez-Montiel, L.G., 2019. Biocontrol of postharvest fruit fungal diseases by bacterial antagonists: a review. Agronomy 9 (3). https://doi.org/10.3390/agronomy9030121.

Carrasco, E., Morales-Rueda, A., García-Gimeno, R.M., 2012. Cross-contamination and recontamination by Salmonella in foods: a review. Food Res. Int. 45 (2), 545–556. https://doi.org/10.1016/j.foodres.2011.11.004.

Carrascosa, C., Raheem, D., Ramos, F., Saraiva, A., Raposo, A., 2021. Microbial biofilms in the food industry—a comprehensive review. Int. J. Environ. Res. Publ. Health 18 (4), 1–31. https://doi.org/10.3390/ijerph18042014.

Chen, H., Wang, J., Cheng, Y., Wang, C., Liu, H., Bian, H., Pan, Y., Sun, J., Han, W., 2019. Application of protein-based films and coatings for food packaging: a review. Polymers 11 (12). https://doi.org/10.3390/polym11122039.

Chen, X., Chen, W., Lu, X., Mao, Y., Luo, X., Liu, G., Zhu, L., Zhang, Y., 2021. Effect of chitosan coating incorporated with oregano or cinnamon essential oil on the bacterial diversity and shelf life of roast duck in modified atmosphere packaging. Food Res. Int. 147, 110491 https://doi.org/10.1016/j.foodres.2021.110491.

Cheng, S.S., Liu, J.Y., Chang, E.H., Chang, S.T., 2008. Antifungal activity of cinnamaldehyde and eugenol congeners against wood-rot fungi. Bioresour. Technol. 99 (11), 5145–5149. https://doi.org/10.1016/j.biortech.2007.09.013.

Cheng, Y., Feng, G., Moraru, C.I., 2019. Micro-and nanotopography sensitive bacterial attachment mechanisms: a review. Front. Microbiol. 10, 410243 https://doi.org/10.3389/fmicb.2019.00191.

Chi, H., Song, S., Luo, M., Zhang, C., Li, W., Li, L., Qin, Y., 2019. Effect of PLA nanocomposite films containing bergamot essential oil, TiO 2 nanoparticles, and Ag nanoparticles on shelf life of mangoes. Sci. Hortic. 249, 192–198. https://doi.org/10.1016/j.scienta.2019.01.059.

Chouhan, S., Sharma, K., Guleria, S., 2017. Antimicrobial activity of some essential oils—present status and future perspectives. Medicines 4 (3), 58. https://doi.org/10.3390/medicines4030058.

Clemente, I., Aznar, M., Silva, F., Nerín, C., 2016. Antimicrobial properties and mode of action of mustard and cinnamon essential oils and their combination against foodborne bacteria. Innovative Food Sci. Emerging Technol. 36, 26–33. https://doi.org/10.1016/j.ifset.2016.05.013.

Cox, H.J., Li, J., Saini, P., Paterson, J.R., Sharples, G.J., Badyal, J.P.S., 2021. Bioinspired and eco-friendly high efficacy cinnamaldehyde antibacterial surfaces. J. Mater. Chem. B 9 (12), 2918–2930. https://doi.org/10.1039/d0tb02379e.

DeFlorio, W., Liu, S., White, A.R., Taylor, T.M., Cisneros-Zevallos, L., Min, Y., Scholar, E. M.A., 2021. Recent developments in antimicrobial and antifouling coatings to reduce or prevent contamination and cross-contamination of food contact surfaces by bacteria. Compr. Rev. Food Sci. Food Saf. 20 (3), 3093–3134. https://doi.org/10.1111/1541-4337.12750dosSantosAlmeida,J.M.

DeFlorio, W., Liu, S., Arcot, Y., Ulugun, B., Wang, X., Min, Y., Cisneros-Zevallos, L., Akbulut, M., 2023. Durable superhydrophobic coatings for stainless-steel: an effective defense against Escherichia coli and Listeria fouling in the post-harvest environment. Food Res. Int. 173, 113227 https://doi.org/10.1016/j.foodres.2023.113227.

dos Santos Almeida, L.A.F., Pascoal, J.L.S., de Almeida, R.R., Guerra, J.H.V., da Silva, D. R.P., da Silva, M.R.S., Neto, T.D.D., Martins, 2021. Effects of dietary L-glutamine and glutamic acid combination, and whey powder on the performance and nutrient digestion in weaned piglets fed grain-based diets. Anim. Biosci. 34, 1963–1973. https://doi.org/10.5713/ab.20.0613.

El-Sakhawy, M., Salama, A., Mohamed, S.A.A., 2023. Propolis applications in food industries and packaging. Biomass Conversion and Biorefinery 1–16. https://doi.org/10.1007/s13399-023-04044-9.

Fei, T., Leyva-Gutierrez, F.M.A., Wan, Z., Wang, T., 2021. Development of a novel soy-wax containing emulsion with enhanced antifungal properties for the postharvest treatment of fresh citrus fruit. Lebensm. Wiss. Technol. 141, 110878 https://doi.org/10.1016/j.lwt.2021.110878.

Fernandes, P.É., São José, J.F.B., Zerdas, E.R.M.A., Andrade, N.J., Fernandes, C.M., Silva, L.D., 2014. Influence of the hydrophobicity and surface roughness of mangoes and tomatoes on the adhesion of Salmonella enterica serovar Typhimurium and evaluation of cleaning procedures using surfactin. Food Control 41 (1), 21–26. https://doi.org/10.1016/j.foodcont.2013.12.024.

Fernández-Muñoz, R., Heredia, A., Domínguez, E., 2022. The role of cuticle in fruit shelf-life. Curr. Opin. Biotechnol. 78, 102802 https://doi.org/10.1016/j.copbio.2022.102802.

Food and Drug Administration, 2023. CFR - Code of Federal Regulations Title 21, Section-175.250. https://www.accessdata.fda.gov/scripts/cdrh/cfdocs/cfcfr/CFRSearch.cfm?fr=175.250.

Gallo, M., Ferrara, L., Calogero, A., Montesano, D., Naviglio, D., 2020. Relationships between food and diseases: what to know to ensure food safety. Food Res. Int. 137, 109414 https://doi.org/10.1016/j.foodres.2020.109414.

Gao, Q., Qi, J., Tan, Y., Ju, J., 2024. Antifungal mechanism of Angelica sinensis essential oil against Penicillium roqueforti and its application in extending the shelf life of bread. Int. J. Food Microbiol. 408, 110427 https://doi.org/10.1016/j.ijfoodmicro.2023.110427.

Gautam, V., Singhal, L., Arora, S., Jha, C., Ray, P., 2013. Reliability of Kirby-Bauer disk diffusion method for detecting carbapenem resistance in Acinetobacter baumannii-calcoaceticus complex isolates. Antimicrob. Agents Chemother. 57 (4), 2003–2004. https://doi.org/10.1128/AAC.01450-12.

Gennes, P., Brochard-Wyart, F., Quéré, D., 2004. Capillarity and Wetting Phenomena. https://doi.org/10.1007/978-0-387-21656-0. Capillarity and Wetting Phenomena.

Global fresh fruits and vegetables market segmented, Market Data Forecast, 2023. https://www.marketdataforecast.com/market-reports/fresh-fruits-and-vegetables-market.

Gomes, D.J.C., De Souza, N.C., Silva, J.R., 2013. Using a monocular optical microscope to assemble a wetting contact angle analyser. Measurement: Journal of the International Measurement Confederation 46 (9), 3623–3627. https://doi.org/10.1016/j.measurement.2013.07.010.

Graça, A., Esteves, E., Nunes, C., Abadias, M., Quintas, C., 2017. Microbiological quality and safety of minimally processed fruits in the marketplace of southern Portugal. Food Control 73, 775–783. https://doi.org/10.1016/j.foodcont.2016.09.046.

Grimaud, R., 2010. Handbook of Hydrocarbon and Lipid Microbiology. https://doi.org/10.1007/978-3-540-77587-4. Handbook of Hydrocarbon and Lipid Microbiology.

Hall, D., 1966. A study of the surface wax deposits on apple fruit. Aust. J. Biol. Sci. 19 (6), 1017. https://doi.org/10.1071/bi9661017.

Hamarsland, H., Nordengen, A.L., Nyvik Aas, S., Holte, K., Garthe, I., Paulsen, G., Cotter, M., Børsheim, E., Benestad, H.B., Raastad, T., 2017. Native whey protein with high levels of leucine results in similar post-exercise muscular anabolic responses as regular whey protein: a randomized controlled trial. Sports Nutr. Rev. J. 14 (1) https://doi.org/10.1186/s12970-017-0202-y.

Hatmaker, E.A., Rangel-Grimaldo, M., Raja, H.A., Pourhadi, H., Knowles, S.L., Fuller, K., Adams, E.M., Lightfoot, J.D., Bastos, R.W., Goldman, G.H., Oberlies, N.H., Rokas, A., 2022. Genomic and phenotypic trait variation of the opportunistic human pathogen Aspergillus flavus and its close relatives. Microbiol. Spectr. 10 (6) https://doi.org/10.1128/spectrum.03069-22.

Hermansson, M., 1999. The DLVO theory in microbial adhesion. Colloids Surf. B Biointerfaces 14 (1–4), 105–119. https://doi.org/10.1016/S0927-7765(99)00029-6.

Joshi, B.L., Graf, R., Gindra, S., Vilgis, T.A., 2021. Effect of different derivatives of paraffin waxes on crystallization of eutectic mixture of cocoa butter-coconut oil. Curr. Res. Food Sci. 4, 784–799. https://doi.org/10.1016/j.crfs.2021.10.010.

Ju, J., Guo, Y., Cheng, Y., Yaoc, W., 2022. Analysis of the synergistic antifungal mechanism of small molecular combinations of essential oils at the molecular level. Ind. Crop. Prod. 188, 115612 https://doi.org/10.1016/j.indcrop.2022.115612.

Ju, J., Lei, Y., Guo, Y., Yu, H., Cheng, Y., Yao, W., 2023. Eugenol and citral kills Aspergillus Niger through the tricarboxylic acid cycle and its application in food preservation. Lebensm. Wiss. Technol. 173, 114226 https://doi.org/10.1016/j.lwt.2022.114226.

Keykhosravi, S.S., 2018. Evaluating the economic and environmental aspects of glass recycling in concrete products in tehran. Journal of Environmental Science Studies 3 (2), 680–692.

Kouassi, K.H.S., Bajji, M., Jijakli, H., 2012. The control of postharvest blue and green molds of citrus in relation with essential oil-wax formulations, adherence and viscosity. Postharvest Biol. Technol. 73, 122–128. https://doi.org/10.1016/j.postharvbio.2012.06.008.

Lai, Y., Lai, J., Wang, S.S., Kuo, Y., Lin, T., 2022. International Journal of Biological Macromolecules Silver nanoparticle-deposited whey protein isolate amyloid fibrils as catalysts for the reduction of methylene blue. Int. J. Biol. Macromol. 213 (March), 1098–1114. https://doi.org/10.1016/j.ijbiomac.2022.06.016.

Li, Y.Q., Kong, D.X., Wu, H., 2013. Analysis and evaluation of essential oil components of cinnamon barks using GC-MS and FTIR spectroscopy. Ind. Crop. Prod. 41 (1), 269–278. https://doi.org/10.1016/j.indcrop.2012.04.056.

Li, B., Wang, H., Xu, J., Qu, W., Yao, L., Yao, B., Yan, C., Chen, W., 2023. Filtration assisted pretreatment for rapid enrichment and accurate detection of Salmonella in vegetables. Food Sci. Hum. Wellness 12 (4), 1167–1173. https://doi.org/10.1016/j.fshw.2022.10.042.

Lin, Y.T., Liu, S., Bhat, B., Kuan, K.Y., Zhou, W., Cobos, I.J., Kwon, J. S. Il, Akbulut, M. S., 2023. pH- and temperature-responsive supramolecular assemblies with highly adjustable viscoelasticity: a multi-stimuli binary system. Soft Matter 19 (29), 5609–5621. https://doi.org/10.1039/d3sm00549f.

Liu, S., Ulugun, B., DeFlorio, W., Arcot, Y., Yegin, Y., Salazar, K.S., Castillo, A., Taylor, T. M., Cisneros-Zevallos, L., Akbulut, M., 2021. Development of durable and superhydrophobic nanodiamond coating on aluminum surfaces for improved hygiene of food contact surfaces. J. Food Eng. 298, 110487 https://doi.org/10.1016/j.jfoodeng.2021.110487.

Livney, Y.D., 2010. Milk proteins as vehicles for bioactives. In: Current Opinion in Colloid and Interface Science, vol. 15. Elsevier, pp. 73–83. https://doi.org/10.1016/j.cocis.2009.11.002. Issues 1–2.

Lo Grasso, A., Fort, A., Mahdizadeh, F.F., Magnani, A., Mocenni, C., 2023. Generalized logistic model of bacterial growth. Math. Comput. Model. Dyn. Syst. 29 (1), 169–185. https://doi.org/10.1080/13873954.2023.2236681.

Lucas-González, R., Yilmaz, B., Mousavi Khaneghah, A., Hano, C., Shariati, M.A., Bangar, S.P., Goksen, G., Dhama, K., Lorenzo, J.M., 2023. Cinnamon: an antimicrobial ingredient for active packaging. In: Food Packaging and Shelf Life, vol. 35. Elsevier Ltd, 101026. https://doi.org/10.1016/j.fpsl.2023.101026.

Lv, Y.M., Elnur, E., Wang, W., Thakur, K., Du, J., Li, H.N., Ma, W.P., Liu, Y.Q., Ni, Z.J., Wei, Z.J., 2022. Hydrogen sulfide treatment increases the antioxidant capacity of fresh Lingwu Long Jujube (Ziziphus jujuba cv. Mill) fruit during storage. Curr. Res. Food Sci. 5, 949–957. https://doi.org/10.1016/j.crfs.2022.05.010.

Maikranz, E., Spengler, C., Thewes, N., Thewes, A., Nolle, F., Jung, P., Bischoff, M., Santen, L., Jacobs, K., 2020. Different binding mechanisms of: Staphylococcus aureus to hydrophobic and hydrophilic surfaces. Nanoscale 12 (37), 19267–19275. https://doi.org/10.1039/d0nr03134h.

Maringgal, B., Hashim, N., Mohamed Amin Tawakkal, I.S., Muda Mohamed, M.T., 2020. Recent advance in edible coating and its effect on fresh/fresh-cut fruits quality. Trends Food Sci. Technol. 96, 253–267. https://doi.org/10.1016/j.tifs.2019.12.024.

Massaglia, S., Borra, D., Peano, C., Sottile, F., Merlino, V.M., 2019. Consumer preference heterogeneity evaluation in fruit and vegetable purchasing decisions using the best–worst approach. Foods 8 (7). https://doi.org/10.3390/foods8070266.

Md Nor, S., Ding, P., 2020. Trends and advances in edible biopolymer coating for tropical fruit: a review. Food Res. Int. 134 https://doi.org/10.1016/j.foodres.2020.109208.

Miranda, M., Sun, X., Marín, A., dos Santos, L.C., Plotto, A., Bai, J., Benedito Garrido Assis, O., David Ferreira, M., Baldwin, E., 2022. Nano- and micro-sized carnauba wax emulsions-based coatings incorporated with ginger essential oil and hydroxypropyl methylcellulose on papaya: preservation of quality and delay of post-harvest fruit decay. Food Chem. X 13, 100249. https://doi.org/10.1016/j.fochx.2022.100249.

Mostafidi, M., Sanjabi, M.R., Shirkhan, F., Zahedi, M.T., 2020. A review of recent trends in the development of the microbial safety of fruits and vegetables. Trends Food Sci. Technol. 103 (April 2019), 321–332. https://doi.org/10.1016/j.tifs.2020.07.009.

Mu, M., Lin, Y.T., DeFlorio, W., Arcot, Y., Liu, S., Zhou, W., Wang, X., Min, Y., Cisneros-Zevallos, L., Akbulut, M., 2023. Multifunctional antifouling coatings involving mesoporous nanosilica and essential oil with superhydrophobic, antibacterial, and bacterial antiadhesion characteristics. Appl. Surf. Sci. 634, 157656 https://doi.org/10.1016/j.apsusc.2023.157656.

Mujika Garai, R., Covián Sánchez, I., Tejera García, R., Rodríguez Valverde, M.A., Cabrerizo Vílchez, M.A., Hidalgo-Álvarez, R., 2005. Study on the effect of raw

material composition on water-repellent capacity of paraffin wax emulsions on wood. J. Dispersion Sci. Technol. 26 (1), 9–18. https://doi.org/10.1081/DIS-200040872.

Muthuselvi, R., Kumar, P.N., Jagathjothi, N., Ramasamy, R., Krishnakumare, B., Suresh, R., Minithra, R., 2020. Importance of Edible wax coatings in fruits and vegetables. Ind. Farm. 7 (11), 1006–1009. https://www.researchgate.net/publication/345308452.

National food and agriculture incident Annex to the Response and recovery federal interagency Operations Plans. https://www.fema.gov/sites/default/files/2020-07/fema_incident_annex_food-agriculture.pdf, 2019.

Oh, J.K., Yegin, Y., Yang, F., Zhang, M., Li, J., Huang, S., Verkhoturov, S.V., Schweikert, E.A., Perez-Lewis, K., Scholar, E.A., Taylor, T.M., Castillo, A., Cisneros-Zevallos, L., Min, Y., Akbulut, M., 2018. The influence of surface chemistry on the kinetics and thermodynamics of bacterial adhesion. Sci. Rep. 8 (1), 1–13. https://doi.org/10.1038/s41598-018-35343-1.

Oliveira Filho, J. G. de, Albiero, B.R., Calisto, Í.H., Bertolo, M.R.V., Oldoni, F.C.A., Egea, M.B., Bogusz Junior, S., de Azeredo, H.M.C., Ferreira, M.D., 2022. Bio-nanocomposite edible coatings based on arrowroot starch/cellulose nanocrystals/carnauba wax nanoemulsion containing essential oils to preserve quality and improve shelf life of strawberry. Int. J. Biol. Macromol. 219, 812–823. https://doi.org/10.1016/j.ijbiomac.2022.08.049.

Orafidiya, L.O., Oyedele, A.O., Shittu, A.O., Elujoba, A.A., 2001. The formulation of an effective topical antibacterial product containing Ocimum gratissimum leaf essential oil. Int. J. Pharm. 224 (1–2), 177–183. https://doi.org/10.1016/S0378-5173(01)00764-5.

Palou, L., Pérez-Gago, M.B., 2021. Antifungal edible coatings for postharvest preservation of fresh fruit. Acta Hortic. 1325, 127–140. https://doi.org/10.17660/ActaHortic.2021.1325.20.

Papadopoulos, P., Mammen, L., Deng, X., Vollmer, D., Butt, H.J., 2013. How superhydrophobicity breaks down. Proc. Natl. Acad. Sci. U.S.A. 110 (9), 3254–3258. https://doi.org/10.1073/pnas.1218673110.

Pashova, S., 2023. Application of plant waxes in edible coatings. Coatings 13 (5), 911. https://doi.org/10.3390/coatings13050911.

Phosanam, A., Moreira, J., Adhikari, B., Adhikari, A., Losso, J.N., 2023. Stabilization of ginger essential oil Pickering emulsions by pineapple cellulose nanocrystals. Curr. Res. Food Sci. 7, 100575 https://doi.org/10.1016/j.crfs.2023.100575.

Purkait, S., Bhattacharya, A., Bag, A., Chattopadhyay, R.R., 2020. Synergistic antibacterial, antifungal and antioxidant efficacy of cinnamon and clove essential oils in combination. Arch. Microbiol. 202 (6), 1439–1448. https://doi.org/10.1007/s00203-020-01858-3.

Rahman, S.M.E., Mele, M.A., Lee, Y.-T., Islam, M.Z., 2021. Consumer preference, quality, and safety of organic and conventional fresh fruits, vegetables, and cereals. Foods 10 (1), 105. https://doi.org/10.3390/foods10010105.

Ravindran, S., Williams, M.A.K., Ward, R.L., Gillies, G., 2018. Understanding how the properties of whey protein stabilized emulsions depend on pH, ionic strength and calcium concentration, by mapping environmental conditions to zeta potential. Food Hydrocolloids 79, 572–578. https://doi.org/10.1016/j.foodhyd.2017.12.003.

Reyes-Jurado, F., Bárcena-Massberg, Z., Ramírez-Corona, N., López-Malo, A., Palou, E., 2022. Fungal inactivation on Mexican corn tortillas by means of thyme essential oil in vapor-phase. Curr. Res. Food Sci. 5, 629–633. https://doi.org/10.1016/j.crfs.2022.03.010.

Rosenberg, M., Kjelleberg, S., 1986. Hydrophobic Interactions: Role in Bacterial Adhesion. Springer, Boston, MA, pp. 353–393. https://doi.org/10.1007/978-1-4757-0611-6_8.

Rosol, T.J., Cohen, S.M., Eisenbrand, G., Fukushima, S., Gooderham, N.J., Guengerich, F. P., Hecht, S.S., Rietjens, I.M.C.M., Davidsen, J.M., Harman, C.L., Kelly, S., Ramanan, D., Taylor, S.V., 2023. FEMA GRAS assessment of natural flavor complexes: lemongrass oil, chamomile oils, citronella oil and related flavoring ingredients. Food Chem. Toxicol. 175, 113697 https://doi.org/10.1016/j.fct.2023.113697.

Ruan, X., Li, P., Wang, C., He, Z., Liu, Y., Zhou, C., Du, L., Song, S., Yang, Z., 2022. Synergistic antibacterial activity of chitosan modified by double antibacterial agents as coating material for fruits preservation. Int. J. Biol. Macromol. 222, 3100–3107. https://doi.org/10.1016/j.ijbiomac.2022.10.084.

Ruiz-Llacsahuanga, B., Hamilton, A.M., Anderson, K., Critzer, F., 2022. Efficacy of cleaning and sanitation methods against Listeria innocua on apple packing equipment surfaces. Food Microbiol. 107, 104061 https://doi.org/10.1016/j.fm.2022.104061.

Rux, G., Labude, C., Herppich, W.B., Geyer, M., 2023. Investigation on the potential of applying bio-based edible coatings for horticultural products exemplified with cucumbers. Curr. Res. Food Sci. 6, 100407 https://doi.org/10.1016/j.crfs.2022.100407.

Sanchez-Tamayo, M., Ruiz-Llacsahuanga, B., Raad, R., Kerr, W., Critzer, F., 2024. Inactivation of foodborne pathogens on gala apples by application of antimicrobial waxes. Food Control 155, 110049. https://doi.org/10.1016/j.foodcont.2023.110049.

Science, F., 1990. Modeling of the bacterial growth curve, 56 (6), 1875–1881.

Sheng, L., Zhu, M.J., 2021. Practical in-storage interventions to control foodborne pathogens on fresh produce. Compr. Rev. Food Sci. Food Saf. 20 (5), 4584–4611. https://doi.org/10.1111/1541-4337.12786.

Stand, M.H.-N., 2020. Using effective hand hygiene practice to prevent and control infection. Mghpcs.Org. https://doi.org/10.7748/ns.2020.e11552.

Tang, C., Zhao, Z., Yang, M., Lu, X., Fu, L., Jiang, G., 2022. Preparation and characterization of sodium cellulose sulfate/chitosan composite films loaded with curcumin for monitoring pork freshness. Curr. Res. Food Sci. 5, 1475–1483. https://doi.org/10.1016/j.crfs.2022.08.019.

Tao, V.X., Tram, T.B., Hien, N.T., Dung, T.H., Tuan, T. Van, 2020. The antifungal activity of essential oils from some plants in Vietnam against the pathogenic fungi Candida albicans and Aspergillus fumigatus. Vietnam Journal of Science, Technology and Engineering 62 (3), 70–75. https://doi.org/10.31276/vjste.62(3).70-75.

Tjørve, K.M.C., Tjørve, E., 2017. The use of Gompertz models in growth analyses, and new Gompertz-model approach: an addition to the Unified-Richards family. PLoS One 12 (6), e0178691. https://doi.org/10.1371/journal.pone.0178691.

Uğur Tutar, İ.K., 2020. Cumhuriyet Science Journal 41 (3), 160–168. Cumhuriyet Science Journal.

Varughese, S.M., Bhandaru, N., 2020. Durability of submerged hydrophobic surfaces. Soft Matter 16 (6), 1692–1701. https://doi.org/10.1039/c9sm01942a.

Wang, H.H., Han, X., Jiang, Y., Wu, G., 2022. Revealed consumers' preferences for fresh produce attributes in Chinese online markets: a case of domestic and imported apples. PLoS One 17 (6), e0270257. https://doi.org/10.1371/journal.pone.0270257.

Wunsch, N.-G., 2023. U.S.: Consumers' preferences for fruits and vegetables by look 2022 | Statista. https://www.statista.com/statistics/1362600/appearance-of-fruits-and-vegetables-to-consumers-in-the-united-states/.

Yaashikaa, P.R., Kamalesh, R., Senthil Kumar, P., Saravanan, A., Vijayasri, K., Rangasamy, G., 2023. Recent advances in edible coatings and their application in food packaging. In: Food Research International, vol. 173. Elsevier Ltd, 113366. https://doi.org/10.1016/j.foodres.2023.113366.

Yadav, V., Heitman, J., 2022. On fruits and fungi: a risk of antifungal usage in food storage and distribution in driving Drug resistance in Candida auris. mBio 13 (3). https://doi.org/10.1128/mbio.00739-22.

Yang, S.-H., Panjaitan, B.P., 2021. A multi-country comparison of consumers' preferences for imported fruits and vegetables. Horticulturae 7 (12), 578. https://doi.org/10.3390/horticulturae7120578.

Yang, S., Mao, X.Y., Li, F.F., Zhang, D., Leng, X.J., Ren, F.Z., Teng, G.X., 2012. The improving effect of spray-drying encapsulation process on the bitter taste and stability of whey protein hydrolysate. Eur. Food Res. Technol. 235 (1), 91–97. https://doi.org/10.1007/s00217-012-1735-6.

Yuan, Y., Hays, M.P., Hardwidge, P.R., Kim, J., 2017. Surface characteristics influencing bacterial adhesion to polymeric substrates. RSC Adv. 7 (23), 14254–14261. https://doi.org/10.1039/c7ra01571b.